Fraunhofer Institut
Techno- und
Wirtschaftsmathematik

C. H. Lampert, O. Wirjadi

An Optimal Non-Orthogonal Separation of the Anisotropic Gaussian Convolution Filter

Berichte des Fraunhofer ITWM, Nr. 82 (2005)

ISSN 1434-9973

Bericht 82 (2005)

Die Veröffentlichungen in der Berichtsreihe des Fraunhofer ITWM können bezogen werden über:

Fraunhofer-Institut für Techno- und
Wirtschaftsmathematik ITWM
Fraunhofer-Platz 1

67663 Kaiserslautern
Germany

Telefon: +49 (0) 6 31/3 16 00-0
Telefax: +49 (0) 6 31/3 16 00-10 99
E-Mail: info@itwm.fraunhofer.de
Internet: www.itwm.fraunhofer.de

Vorwort

Das Tätigkeitsfeld des Fraunhofer Instituts für Techno- und Wirtschaftsmathematik ITWM umfasst anwendungsnahe Grundlagenforschung, angewandte Forschung sowie Beratung und kundenspezifische Lösungen auf allen Gebieten, die für Techno- und Wirtschaftsmathematik bedeutsam sind.

In der Reihe »Berichte des Fraunhofer ITWM« soll die Arbeit des Instituts kontinuierlich einer interessierten Öffentlichkeit in Industrie, Wirtschaft und Wissenschaft vorgestellt werden. Durch die enge Verzahnung mit dem Fachbereich Mathematik der Universität Kaiserslautern sowie durch zahlreiche Kooperationen mit internationalen Institutionen und Hochschulen in den Bereichen Ausbildung und Forschung ist ein großes Potenzial für Forschungsberichte vorhanden. In die Berichtreihe sollen sowohl hervorragende Diplom- und Projektarbeiten und Dissertationen als auch Forschungsberichte der Institutsmitarbeiter und Institutsgäste zu aktuellen Fragen der Techno- und Wirtschaftsmathematik aufgenommen werden.

Darüberhinaus bietet die Reihe ein Forum für die Berichterstattung über die zahlreichen Kooperationsprojekte des Instituts mit Partnern aus Industrie und Wirtschaft.

Berichterstattung heißt hier Dokumentation darüber, wie aktuelle Ergebnisse aus mathematischer Forschungs- und Entwicklungsarbeit in industrielle Anwendungen und Softwareprodukte transferiert werden, und wie umgekehrt Probleme der Praxis neue interessante mathematische Fragestellungen generieren.

Prof. Dr. Dieter Prätzel-Wolters
Institutsleiter

Kaiserslautern, im Juni 2001

An Optimal Non-Orthogonal Separation of the Anisotropic Gaussian Convolution Filter

Christoph H. Lampert* and Oliver Wirjadi†

October 24, 2005

Abstract

We give an analytical and geometrical treatment of what it means to separate a Gaussian kernel along arbitrary axes in $\mathbb{R}^n$, and we present a separation scheme that allows to efficiently implement anisotropic Gaussian convolution filters in arbitrary dimension. Based on our previous analysis we show that this scheme is optimal with regard to the number of memory accesses and interpolation operations needed.

Our method relies on non-orthogonal convolution axes and works completely in image space. Thus, it avoids the need for an FFT-subroutine. Depending on the accuracy and speed requirements, different interpolation schemes and methods to implement the one-dimensional Gaussian (FIR, IIR) can be integrated. The algorithm is also feasible for hardware that does not contain a floating-point unit.

Special emphasis is laid on analyzing the performance and accuracy of our method. In particular, we show that without any special optimization of the source code, our method can perform anisotropic Gaussian filtering faster than methods relying on the Fast Fourier Transform.

Keywords

Anisotropic Gaussian filter, linear filtering, orientation space, nD image processing, separable filters

1 Introduction

1.1 Anisotropic Gaussian Filtering

Gaussian convolution filters are frequently used tools in one- and multidimensional signal processing. The exponential decay of their kernels in the signal domain as well as in the frequency domain and their strict positiveness make them very well behaved low pass filters. While one-dimensional Gaussian filters are completely described by a single variance parameter, in multidimensional applications, like image processing, Gaussian filters can have different shapes. The most frequently used are isotropic ones, but the reason for this is mainly historical, because isotropic Gaussian filters also have only one free (variance) parameter. This makes them easy to handle analytically, and simple and fast to implement.

*C.H. Lampert is with with the Image Understanding and Pattern Recognition Group at the German Research Center for Artificial Intelligence (DFKI) GmbH, 67663 Kaiserslautern, Germany, telephone: +49–631–2053363, fax: +49–631–2053357, e–mail: chl@iupr.net

†O. Wirjadi is with the Models and Algorithms in Image Processing Group at the Fraunhofer ITWM, 67663 Kaiserslautern, Germany, telephone: +49–631–3031874, fax: +49–631–3031811, e–mail: oliver.wirjadi@itwm.fraunhofer.de

From the signal and image processing point of view, anisotropic Gaussians are much more interesting, because their additional parameters encode information about orientation as well as scale. During the last years a tendency towards anisotropic filtering has become visible in many areas. Often one can rely on local image information, like gradient directions, to build anisotropic filters, allowing smoothing and de-noising while preserving edges [1, 2]. Wang et al. propose the use of local covariance estimates to build anisotropic kernels for adaptive video segmentation based on the mean shift procedure [3]. This relies on the fact that from a probabilistic view anisotropic Gaussians can express correlations between different signal directions, while isotropic Gaussians are based on the often unrealistic assumption that all quantities involved are statistically independent.

Also if local orientation is not known a priori, anisotropic filters often prove useful. By arranging many such filters with different orientations and variances in form of a filter bank, local orientations of line and surface structures can be deduced, see [4, 5, 6, 7]. This approach is often referred to as *orientation space theory* [8], in analogy to the *scale space theory* of isotropic Gaussians [9]. Detecting and enhancing structure using orientation spaces is of particular interest in 3D imaging, e.g. medical, where no established feature extraction method like the classical 2D Canny edge detector is available.

Anisotropic filtering also has attracted interest in other areas, even in hardware design and visualization. All modern graphics processing units (GPUs) contain dedicated units for anisotropic filtering, allowing visualization effects like adaptive motion blur to be applied in real time [10].

We believe that if today anisotropic Gaussian filters have not become a standard tool in image and signal processing in the same way that isotropic ones have, then this is because there is no established way how to efficiently implement them. It it well known that isotropic Gaussian filters can always be separated, i.e. their n-dimensional convolution integral can be implemented as a sequence of n one-dimensional convolutions along the coordinate axes. For general anisotropic Gaussians this is not possible. Although they as well can be separated along their main axes, decomposing the n-dimensional integral into n one-dimensional ones, the directions of integration then are rotated with respect to the coordinate grid, making this form of implementation cumbersome and slow. Instead, it is usually faster to utilize the Fourier Convolution Theorem to do the filtering: the signal is Fourier transformed, multiplied with the transformed convolution kernel, and transformed back using the inverse Fourier transform. This requires more memory and computational effort than in the isotropic case, and also usually the inclusion of a mathematical library providing the Fast Fourier Transform (FFT). Also, since the FFT is a global operation, the whole image is processed at once, and local filtering of just a small window of the image is not as easy as when working directly with the image data. Another drawback is that the FFT cannot cope with missing sample data, and it requires a CPU capable of performing floating-point operations.

Freeman and Adelson showed in [11] that it is not possible to construct a steerable basis for the rotated Gaussians, and even for an approximate solution as found by Perona in 1992 [12], the basis turned out to be too large for practical use. Also, the basis functions are not separable themselves, and thus cannot be implemented in an efficient way.

Only in the year 2002, Geusebroek and Smeulders came up with an efficient scheme to separate anisotropic Gaussians in $\mathbb{R}^2$ [13, 14]: their idea was to keep one direction of convolution fixed (and usually axis-aligned), but to allow the other directions to vary depending on the parameters of the Gaussian. The method does not yield orthogonal filtering directions, but allows for an efficient implementation. Using the recursive approximation scheme for 1D-Gaussian convolutions, as proposed by Young [15], the result is an algorithm that is faster than the Fourier-based

one, achieving $O(1)$ complexity per pixel.

Based on this approach, Wirjadi and Breuel in 2005 gave an approximate formula in a special case in $\mathbb{R}^3$ [16]. They fix two directions to be axis aligned, while the third varies with the Gaussian parameters. This again allows for a fast implementation, but only for few filter directions the approximation is good enough to be used in practice.

1.2 Our Contribution

Our goal in this paper is to fill the gap that still exists for dimensions larger than 2. We develop an intuitive, geometrically motivated theory of what it means to separate a Gaussian kernel along arbitrary axes in $\mathbb{R}^n$. From these consideration, we derive a separation scheme for anisotropic Gaussians which is optimal in the sense of the number of memory accesses and interpolation operations required.

To allow its application in real life problems, we concretize our result for the most important cases in image processing: in $\mathbb{R}^2$, our result turns out to be identical to the separation by Geusebroek and Smeulders, showing the optimality of their result in this case. For Gaussians in $\mathbb{R}^3$ with two identical covariance values, we give explicit formulas, parameterized by the variances and major axes of the Gaussians. In the general case, a simple numerical method based on the Cholesky decomposition is derived.

To further demonstrate the method proposed, we implemented it in plain C and applied it to a number of typical situations in image processing of 2D and 3D data. This makes it possible to present visual output as well as thorough results on accuracy and efficiency.

The rest of the paper is structured as follows:

Section 2 studies the general form of how to separate the Gaussian convolution kernel. Section 3 presents two examples of such separations, the classical one based on the Singular Value Decomposition, and the one favored in this paper, relying on a Triangular Factorization of Cholesky Type. In Section 4 the latter is calculated explicitly in $\mathbb{R}^2$ and the most frequently needed cases of $\mathbb{R}^3$. In $\mathbb{R}^n$ a numerical way to calculate the separation coefficients is explained. Also, a geometrical interpretation of the separations is given, which sheds light on how and why the algorithm works the way it does. Section 5 deals with the issues of implementing the theoretical results, in particular the question of how to discretize and interpolate the continuous operators. In Section 6 and 7, runtime and accuracy of the proposed filter setup are examined, comparing them to the FFT-based approach. Section 8 presents some applications of the algorithm to real life problems. Finally, Section 9 summarizes the results achieved and discusses current limitations and possible extensions and improvements of the method.

2 The Gaussian Convolution Integral

2.1 Factorization of the Gaussian

The steps how to factorize an isotropic Gaussian along the coordinate axes are classical. In some areas, e.g. statistical pattern recognition, also the separation of possibly anisotropic Gaussians along their main orthogonal axes is a standard procedure, usually in the setup of the 'whitening transform', see e.g. [17, Ch. 2]. In this section, however, we will study the much more general concept of if and how a Gaussian convolution filter can be separated along arbitrary, possibly non-orthogonal axes in $\mathbb{R}^n$. Our main result is the following:

For any decomposition $\Sigma = VDV^t$ of the covariance matrix Σ into square matrices D and V, where D is diagonal and positive, and V has determinant 1, there is a separation of the nD-Gaussian into 1D-Gaussians, where the separation directions are given by the column vectors of V.

In Section 3, we will see that many such decompositions exist, with or without orthogonal directions, and we will study their properties with regard to an efficient implementation of the Gaussian filter.

To prove the result itself, we first fix some notation. Unless specified otherwise, all our calculations will take place in $\mathbb{R}^n$ where $\mathbf{x} = (x_1, \ldots, x_n)$ and $\mathbf{y} = (y_1, \ldots, y_n)$ are n-dimensional coordinate vectors with respect to the standard Euclidean coordinate system. By $\mathrm{Fun}(X, Y)$ we denote the space of functions from some set X to some set Y. The anisotropic Gaussian filter kernel $g(\mathbf{x}) \in \mathrm{Fun}(\mathbb{R}^n, \mathbb{R})$ with mean 0 and covariance matrix $\Sigma \in \mathbb{R}^{n\times n}$ then has the form

$$g(\mathbf{x}) = \frac{1}{(2\pi)^{n/2}|\Sigma|^{1/2}} \exp\left\{-\frac{1}{2}\mathbf{x}^t\Sigma^{-1}\mathbf{x}\right\}, \tag{1}$$

where $|\Sigma|$ is the determinant of Σ. Our goal is now to find a separation, i.e. to write g as a product of one-dimensional Gaussians. Assume for the moment that a decomposition $\Sigma = VDV^t$ as described above is given. Then $\Sigma^{-1} = V^{-t}D^{-1}V^{-1}$, and we can rewrite the Gaussian to

$$= \frac{\exp\left\{-\frac{1}{2}\mathbf{x}^t(V^{-t}D^{-1}V^{-1})\mathbf{x}\right\}}{(2\pi)^{n/2}|D|^{1/2}}, \tag{2}$$

where we also used that $|D| = |\Sigma|$, which follows from $|V| = 1$. Rewriting the numerator yields

$$= \frac{\exp\left\{-\frac{1}{2}(V^{-1}\mathbf{x})^tD^{-1}(V^{-1}\mathbf{x})\right\}}{(2\pi)^{n/2}|D|^{1/2}}. \tag{3}$$

After a linear change of coordinates from $\mathbf{x}$ to $\mathbf{v} = (v_1, \ldots, v_n)$ with $\mathbf{v} := V^{-1}\mathbf{x}$ this becomes

$$= \frac{1}{(2\pi)^{n/2}|D|^{1/2}} \exp\left\{-\frac{1}{2}\mathbf{v}^tD^{-1}\mathbf{v}\right\}. \tag{4}$$

D is known to be a diagonal matrix with positive entries, which we will denote by $d_1^2, \ldots, d_n^2$, such that $|D|^{1/2} = d_1 \cdot \ldots \cdot d_n$. It follows that D^{-1} is diagonal with positive entries as well, namely $D^{-1} = \mathrm{diag}(\frac{1}{d_1^2}, \ldots, \frac{1}{d_n^2})$. Therefore, the matrix product is in fact just a weighted sum of squares

$$= \frac{1}{(2\pi)^{n/2}d_1 \cdot \ldots \cdot d_n} \exp\left\{-\frac{1}{2}\sum_{i=1}^{n}\frac{v_i^2}{d_i^2}\right\}, \tag{5}$$

which we can split up using the addition theorem for the exponential function

$$= \frac{1}{\sqrt{2\pi}d_1}\exp(-\frac{1}{2}\frac{v_1^2}{d_1^2}) \cdot \ldots \cdot \frac{1}{\sqrt{2\pi}d_n}\exp(-\frac{1}{2}\frac{v_n^2}{d_n^2}). \tag{6}$$

From this we see that using the v-coordinate vector gives us the desired product structure

$$= g_1(v_1) \cdot \ldots \cdot g_n(v_n) \tag{7}$$

where each

$$g_i(v_i) := \frac{1}{\sqrt{2\pi} d_i} \exp\left(-\frac{1}{2}\frac{v_i^2}{d_i^2}\right) \tag{8}$$

is an ordinary 1-dimensional Gaussian of mean 0 and variance d_i^2.

2.2 Separating the Convolution Integral

To see how this factorization of the Gaussian kernel gives rise to a separation of the Gaussian filter, we study what happens to a convolution integral when applying the aforementioned change of coordinates.

For a general function $f \in \mathrm{Fun}(\mathbb{R}^n, \mathbb{R})$, the convolution with the Gaussian $g \in \mathrm{Fun}(\mathbb{R}^n, \mathbb{R})$ is defined as

$$(f * g)(\mathbf{x}) := \int_{\mathbb{R}} \int_{\mathbb{R}} \dots \int_{\mathbb{R}} f(\mathbf{y}) g(\mathbf{x} - \mathbf{y}) \; dy_1 \, dy_2 \, \dots \, dy_n. \tag{9}$$

Changing the coordinates as above, from $\mathbf{x}$ to $\mathbf{u} := V^{-1}\mathbf{x}$ and from $\mathbf{y}$ to $\mathbf{v} := V^{-1}\mathbf{y}$, we obtain

$$= \int_{\mathbb{R}} \dots \int_{\mathbb{R}} \int_{\mathbb{R}} f(V\mathbf{v}) g\left(V\mathbf{u} - V\mathbf{v}\right) |V^{-1}| \; dv_1 \, dv_2 \, \dots \, dv_n, \tag{10}$$

where the factor $|V^{-1}|$ enters from the rules for coordinate changes in integration theory. Using the separation formula (7) and $|V| = 1$, we can rewrite this as

$$\begin{aligned} = \int_{\mathbb{R}} g_n(u_n - v_n) \int_{\mathbb{R}} g_{n-1}(u_{n-1} - v_{n-1}) \dots \\ \int_{\mathbb{R}} g_1(u_1 - v_1) f(V\mathbf{v}) \; dv_1 \, dv_2 \, \dots \, dv_n. \end{aligned} \tag{11}$$

This is the standard form of a separated convolution integral. To better understand what the formula means in practice, we additionally split up the matrix-vector product $V\mathbf{v} = \sum_i v_i \mathbf{v}^i$, such that

$$\begin{aligned} = \int_{\mathbb{R}} g_n(u_n - v_n) \int_{\mathbb{R}} g_{n-1}(u_{n-1} - v_{n-1}) \dots \\ \int_{\mathbb{R}} g_1(u_1 - v_1) f\big(\sum_i v_i \mathbf{v}^i\big) \; dv_1 \, dv_2 \, \dots \, dv_n, \end{aligned} \tag{12}$$

where the $\mathbf{v}^i$ are the columns of the matrix V. Integration over v_i therefore means convolution along the direction $\mathbf{v}^i$. This can be written very compactly using the notation of *directional convolutions*

$$= g_n *_{\mathbf{v}^n} \dots g_2 *_{\mathbf{v}^2} g_1 *_{\mathbf{v}^1} f, \tag{13}$$

where the *directional convolution operator* $*_{\mathbf{v}} : \mathrm{Fun}(\mathbb{R}, \mathbb{R}) \times \mathrm{Fun}(\mathbb{R}^n, \mathbb{R}) \to \mathrm{Fun}(\mathbb{R}^n, \mathbb{R})$ is defined by

$$(g *_{\mathbf{v}} f)(\mathbf{x}) := \int_{-\infty}^{\infty} g(\lambda) f(\mathbf{x} - \lambda\mathbf{v}) \; d\lambda. \tag{14}$$

Note that the integration is one-dimensional, even though the direction is specified by a vector $\mathbf{v} \in \mathbb{R}^n$.

3 Symmetric Factorizations of Σ

The result of the previous section was that any anisotropic Gaussian is separable if we find a decomposition of the covariance matrix of a form $\Sigma = VDV^t$. We call this a *symmetric factorization*. For symmetric and positive definite matrices Σ – as covariance matrices always are – these can be constructed using elementary matrix operations, see [18, Ch. 1]. In fact, there even are many of those with different properties, two of which we will review here: the *Singular Value Decomposition* and the *Triangular Factorization of Cholesky Type*. Our result will be that the latter is more suitable for implementing the Gaussian filter in a discrete setting.

3.1 Singular Value Decomposition

In its general form, the singular value decomposition (SVD) of a symmetric matrix A is $A = VDV^t$, where V is a rotation matrices, and D is diagonal, thus qualifying the SVD as a symmetric factorization. Because V is a rotation matrix, its column vectors are orthogonal to each other and each of length 1. They point into the directions of the axes of the hyper-ellipsoid described by $\{\mathbf{x} : \mathbf{x}^t\Sigma^{-1}\mathbf{x} = 1\}$. Using our previous result that we can separate the Gaussian along the columns of V, this reproves the well-known fact that an anisotropic Gaussian is always separable along its major axes.

However, this approach has major problems for practical purposes, because in case of a general Gaussian, all axes lie rotated in $\mathbb{R}^n$. To filter along these axes, we have to use interpolation in all n dimensions during each of the n integration steps. While this is no problem from the mathematical side, in practice it makes the calculation on a computer slow, and numerical errors can occur and accumulate.

3.2 Triangular Factorization of Cholesky Type

Our motivation for studying other decompositions is to find a factorization $\Sigma = VDV^t$ which gives rise to an algorithm which requires fewer interpolation steps than when relying on the SVD. From Equation (12) we know that interpolation is necessary for convolutions when using the columns of V as directions. Therefore, at first we will study which choices of direction vectors $\mathbf{v}$ have a fast and numerically well-behaved convolution operator $*_{\mathbf{v}}$:

- The simplest case is when $\mathbf{v}$ is a standard unit vector of the Euclidean coordinate system, e.g. $\mathbf{v} = (1, 0, 0, \ldots, 0)$. This results in an axis parallel convolution and no interpolation is necessary.
- If $\mathbf{v}$ lies in a plane spanned by two Euclidean coordinate axes, e.g. $\mathbf{v} = (v_1, v_2, 0, \ldots, 0)$, then only a 2D-interpolation step is necessary per sample. If even $v_1 = 1$ or $v_2 = 1$, interpolation is necessary only 1-dimensionally, because with respect to the other directions the target locations lie on the sampling grid.
- For a general vector $\mathbf{v} = (v_1, v_2, \ldots, v_n)$, the discrete convolution has to perform an n-dimensional interpolation for each sample point. But, if one of the v_i is 1, the interpolation dimension is at least reduced to $n - 1$.

The directions resulting from a general SVD fall under the worst case described above, each requiring n-dimensional interpolation. Also, none of their vector components can be of integer value, since the length of the direction vectors is known to be 1. Instead, we design a factorization with as many zero components in the direction vectors $\mathbf{v}^i$ as possible. Whenever an entry cannot be made 0, we at least try to make it 1.

Since Σ is a symmetric $n \times n$-matrix, it has $\frac{n(n+1)}{2}$ degrees of freedom. Any factorization into V and D will need to have at least as many degrees of freedom as well. n of those go into diagonal entries of D. Therefore, at least $\frac{n(n-1)}{2}$ entries of V will have to remain free. The $\frac{n(n+1)}{2}$ other entries of V we should be able to make either 0 or 1 while adhering the condition that V must have determinant 1.

One decomposition that realizes this dimensional analysis bound is the Triangular Factorization of Cholesky type, see [19, Ch. I]. Starting from the Cholesky decomposition $\Sigma = UU^t$ with upper triangular U, we set $D := \operatorname{diag}(u_{11}^2, \ldots, u_{nn}^2)$ where the u_{ii} are the diagonal entries of U, and $V := D^{-1/2}U$. Then it follows that $\Sigma = VDV^t$ with V an *upper triangular matrix with unit diagonal*.

$$V = \begin{pmatrix} 1 & v_{1,2} & v_{1,3} & \cdots & v_{1,n} \\ & 1 & v_{2,3} & \cdots & v_{2,n} \\ & & \ddots & & \vdots \\ & & & 1 & v_{n-1,n} \\ & & & & 1 \end{pmatrix} \tag{15}$$

In the implementation of equation (12), this means that the convolution along $\mathbf{v}^1$ can be calculated without need for interpolation. Along $\mathbf{v}^2$, one-dimensional interpolation in x_1-direction is necessary etc. until for $\mathbf{v}^n$, $(n-1)$-dimensional interpolation in $x_1, \ldots, x_{n-1}$ has to be performed for each sample. There is never any interpolation required in the x_n variable. Each of the convolution steps requires fewer interpolation steps than any one in the SVD-based separation scheme.

This choice of V in (15) is optimal for the conditions defined above because it contains exactly $\frac{n(n-1)}{2}$ free variables, its diagonal contains ones, thus making its determinant 1, and all remaining entries are 0.

3.3 Calculation of the Triangular Factorization

After having seen that the Triangular Factorization has the potential to give rise to an efficient separation of the anisotropic Gaussian, we examine how to compute it for a given Σ. In parallel to the most important applications, we study the cases of $n = 2$, $n = 3$, and arbitrary n separately.

3.3.1 Explicit Formulas in $\mathbb{R}^2$

The triangular factorization can easily be calculated in closed form by writing down the 2×2 matrices involved

$$V = \begin{pmatrix} 1 & v_{1,2} \\ 0 & 1 \end{pmatrix} \text{ and } D = \begin{pmatrix} d_1^2 & 0 \\ 0 & d_2^2 \end{pmatrix} \tag{16}$$

where $v_{1,2}$, d_1^2 and d_2^2 are the unknown parameters. From this we obtain

$$VDV^t = \begin{pmatrix} d_1^2 + d_2^2 v_{1,2}^2 & d_2^2 v_{1,2} \\ d_2^2 v_{1,2} & d_2^2 \end{pmatrix}. \tag{17}$$

For any positive definite symmetric matrix

$$\Sigma = \begin{pmatrix} s_{1,1} & s_{1,2} \\ s_{1,2} & s_{2,2} \end{pmatrix} \tag{18}$$

we can rewrite the factorization equation $\Sigma = VDV^t$ component wise, and by solving for the unknowns we obtain

$$v_{1,2} = \frac{s_{1,2}}{s_{2,2}}, \quad d_1^2 = s_{1,1} - \frac{s_{1,2}^2}{s_{2,2}}, \quad d_2^2 = s_{2,2}. \tag{19}$$

Because Σ is positive definite, it is ensured that $s_{2,2} > 0$ and $s_{1,1}s_{2,2} - s_{1,2}^2 > 0$. Therefore, all expressions are well defined. We also see that

$$d_1^2 d_2^2 = s_{1,1}s_{2,2} - s_{1,2}^2 \tag{20}$$

which is the explicit formulation in $\mathbb{R}^2$ of the fact that $|D| = |\Sigma|$.

3.3.2 Explicit Formulas in $\mathbb{R}^3$

For 3×3 matrices, the Triangular Factorization can be calculated explicitly in the same way, but one has to deal with more unknowns which complicates the formulas: We write $\Sigma = (s_{i,j})_{i,j=1,2,3}$ with $s_{i,j} = s_{j,i}$, $D = \operatorname{diag}(d_1^2, d_2^2, d_3^2)$ and $V = (v_{i,j})_{i,j=1,2,3}$ with $v_{i,i} = 1$ and $v_{i,j} = 0$ for $i > j$. Now as before solving the system of equations deriving from the individual components of $\Sigma = VDV^t$ yields

$$d_1^2 = s_{1,1} - \frac{(s_{1,2}s_{3,3} - s_{1,3}s_{2,3})^2}{s_{3,3}(s_{2,2}s_{3,3} - s_{2,3}^2)} - \frac{s_{1,3}}{s_{3,3}}, \tag{21}$$

$$d_2^2 = s_{2,2} - \frac{s_{2,3}^2}{s_{3,3}}, \qquad d_3^2 = s_{3,3}, \tag{22}$$

$$v_{1,2} = \frac{s_{1,2}s_{3,3} - s_{1,3}s_{2,3}}{s_{2,2}s_{3,3} - s_{2,3}^2}, \qquad v_{1,3} = \frac{s_{1,3}}{s_{3,3}}, \qquad v_{2,3} = \frac{s_{1,2}}{s_{3,3}}. \tag{23}$$

Note that instead of using Equation (21), it is often more convenient to utilize that $d_1^2 d_2^2 d_3^2 = |\Sigma|$.

3.3.3 Numerical Factorization

In higher dimensions, it is still possible but not practical to derive a closed formula for the factorization matrices depending on the entries of Σ. Instead, V and D can efficiently be calculated using numerical methods. Since this only has to be done once for the filter kernel and not for each pixel, the computational effort is negligible. Some numerical libraries provide a dedicated routine for calculating the Triangular Factorization, otherwise it is possible to obtain it from the Cholesky decomposition as described in Section 3.2.

3.4 Geometrical Interpretation

To understand how the Triangular Factorization really works, it is useful to look at it from a geometrical point of view. Finding a separation of the Gaussian can be thought of in the following way: we perform a linear transformation (namely V^{-1}) on the signal, filter with Gaussians along the coordinate axes, and transform the signal back using the transform V. From this it is seen that the directions of convolution in (12) are the V-transformations of the Euclidean coordinate axes.

This is better visualized geometrically in 2D using ellipses. Ellipses are the contour lines of Gaussians, and each ellipse uniquely corresponds to a Gaussian kernel and vice versa, if we fix the contour ellipse to lie at half of the Gaussian's maximum value.

3.4.1 SVD

It is well known that each ellipse can be made axis-parallel by rotating it. This is how the SVD-based method works: the above mentioned linear transform is a rotation, mapping the ellipses' main axes onto the coordinate axes. After rotating back, this yields convolution directions which are orthogonal to each other, and rotated with respect to the Euclidean frame. See Figure 1b for an illustration.

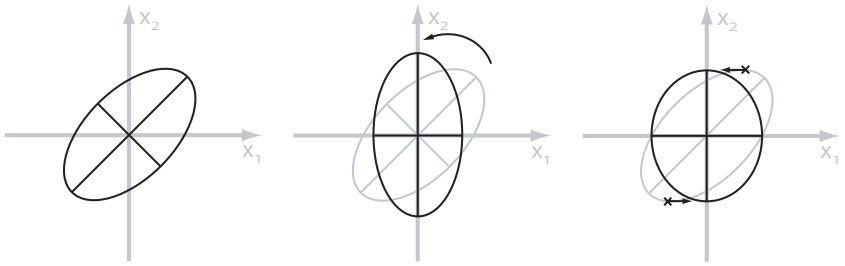

(a) (b) (c)

Figure 1: (a) Any ellipse in the 2D plane can be transformed into an axis-aligned ellipse by using either a (b) rotation or (c) shear.

3.4.2 Triangular Factorization

Each ellipse can also be made axis-parallel by a shear of the y-axis, keeping the x-axis fixed, see Figure 1c. This means that after transforming the signal back, one convolution direction still is the x-axis itself, while the other is a sheared version of the y-axis, intersecting the original ellipsis in its highest point.

4 Anisotropic Gaussian Filtering in Image and Signal Processing

In practice Σ is often not given explicitly, but implicitly by specifying a number of directions in which the Gaussian filtering should take place, and covariance values which give the filter strength. The covariance matrix then is obtained as $\Sigma = R^t S R$, where the direction vectors form the columns of R, and S is a diagonal matrix containing the variance values. In most cases, the directions are not given as vectors, but from a number of rotation angles. In this section, we give formulas for the parameters $\mathbf{v}^i$ and d_i^2, directly parameterized by such rotation angles.

Although we have laid out the theory in arbitrary dimension, in this section we restrict ourselves to two- and special cases of three-dimensional filtering. Other cases are of little practical interest in image processing, and we believe that deriving a (complicated) parameterization for them would not yield any additional insight.

4.1 Parameterizations for Image Processing in 2D

At first, we study Gaussians in $\mathbb{R}^2$ with coordinates (x_1, x_2). A Gaussian is then uniquely determined by an angle θ, specifying the major filtering direction, and the two variances σ_1^2, σ_2^2. Its covariance matrix then is $\Sigma = R_\theta^t S R_\theta$ with

$$R_\theta = \begin{pmatrix} \cos\theta & -\sin\theta \\ \sin\theta & \cos\theta \end{pmatrix} \quad S = \begin{pmatrix} \sigma_1^2 & 0 \\ 0 & \sigma_2^2 \end{pmatrix}. \tag{24}$$

Multiplying this out, we obtain as a general parameterization:

$$\Sigma = \begin{pmatrix} \sigma_1^2 \cos^2\theta + \sigma_2^2 \sin^2\theta & (\sigma_2^2 - \sigma_1^2)\cos\theta\sin\theta \\ (\sigma_2^2 - \sigma_1^2)\cos\theta\sin\theta & \sigma_1^2 \sin^2\theta + \sigma_2^2 \cos^2\theta \end{pmatrix}. \tag{25}$$

Using equation (19), we obtain that Σ's triangular factor matrices are

$$V = \begin{pmatrix} 1 & \frac{(\sigma_2^2-\sigma_1^2)\cos\theta\sin\theta}{\sigma_1^2\sin^2\theta+\sigma_2^2\cos^2\theta} \\ 0 & 1 \end{pmatrix}, \tag{26}$$

$$D = \begin{pmatrix} \frac{\sigma_1^2\sigma_2^2}{\sigma_1^2\cos^2\theta+\sigma_2^2\sin^2\theta} & 0 \\ 0 & \sigma_1^2\cos^2\theta+\sigma_2^2\sin^2\theta \end{pmatrix}. \tag{27}$$

Introducing φ to denote the angle between V's column vectors, i.e. $\varphi = \measuredangle(\mathbf{v}^1, \mathbf{v}^2)$ or

$$\tan\varphi = \frac{\sigma_1^2\sin^2\theta + \sigma_2^2\cos^2\theta}{(\sigma_2^2-\sigma_1^2)\cos\theta\sin\theta}, \tag{28}$$

we have separated the Gaussian into a convolution along the x-axis, and a convolution with direction vector $\mathbf{v}^2 = (\cot\varphi, 1)^t$. The corresponding Gaussian variances are

$$d_1^2 = \frac{\sigma_1^2\sigma_2^2}{\sigma_1^2\cos^2\theta + \sigma_2^2\sin^2\theta}, \tag{29}$$

$$d_2^2 = \sigma_1^2\cos^2\theta + \sigma_2^2\sin^2\theta. \tag{30}$$

This is exactly the result from [14], showing that our theory is in fact an generalization of the work by Geusebroek et al.

4.2 Parameterizations for Image Processing in 3D

In $\mathbb{R}^3$ with coordinates (x_1, x_2, x_3), several ways of specifying the Gaussian from angles are possible. Typically, the construction itself can be thought of as starting with an axis aligned anisotropic Gaussian, and rotating it in $\mathbb{R}^3$ to its target orientation. Our method of choice is based on Euler angles, see [20]. The total rotation matrix is constructed from at most three elementary rotations about the x_1-axis, x_3-axis and again the x_1-axis, i.e.

$$R(\psi, \theta, \varphi) = R_{x_1}(\psi)R_{x_3}(\theta)R_{x_1}(\varphi), \tag{31}$$

where R_{x_1} and R_{x_3} denote the usual rotation matrices about the x_1 and x_3 axes, and $\psi \in [0, \pi[, \theta \in [0, \frac{\pi}{2}]$ and $\varphi \in [0, \pi[$ are the corresponding rotation angles. It is now possible to follow the same track as in $\mathbb{R}^2$: calculate $\Sigma = R^t S R$ explicitly and solve the system of equations that result from $\Sigma = VDV^t$ by using the Equations (21) to (23).

However, the resulting formulas get very long and are not instructive. We will instead only treat a special case which is of most importance in 3D image processing: when detecting lower dimensional structures in three-dimensional data, the anisotropic Gaussian is typically chosen with $\sigma_2 = \sigma_3$. Filtering with $\sigma_1 > \sigma_2$ then means to filter with a prolate rotational ellipsoid, which corresponds to objects that mainly have one-dimensional extent. Filtering with $\sigma_1 < \sigma_2$ turns the Gaussian into the the shape of an oblate rotational ellipsoid, which is useful for searching two-dimensional objects.

For us, choosing $\sigma_2 = \sigma_3$ has the additional advantage that the Gaussian is rotationally invariant to its first axis. With Euler angles, this means that the first rotation in x_1-direction can be dropped from Equation (31), and Σ ends up depending only on four parameters: two rotation angles θ and φ and two variances

σ_1 and σ_2. In detail, this is

$$\Sigma = \begin{pmatrix} \sigma_1^2+(\sigma_2^2-\sigma_1^2)\sin^2\theta & (\sigma_2^2-\sigma_1^2)\cos\varphi\cos\theta\sin\theta & -(\sigma_2^2-\sigma_1^2)\sin\varphi\cos\theta\sin\theta \\ (\sigma_2^2-\sigma_1^2)\cos\varphi\cos\theta\sin\theta & \sigma_2^2-(\sigma_2^2-\sigma_1^2)\cos^2\varphi\sin^2\theta & (\sigma_2^2-\sigma_1^2)\cos\varphi\sin\varphi\sin^2\theta \\ -(\sigma_2^2-\sigma_1^2)\sin\varphi\cos\theta\sin\theta & (\sigma_2^2-\sigma_1^2)\cos\varphi\sin\varphi\sin^2\theta & \sigma_2^2-(\sigma_2^2-\sigma_1^2)\sin^2\varphi\sin^2\theta \end{pmatrix} \tag{32}$$

After elementary but tedious computation we obtain the parameterization:

$$d_1^2 = \frac{\sigma_1^2\sigma_2^2}{\sigma_2^2\cos^2\theta + \sigma_1^2\sin^2\theta} \tag{33}$$

$$d_2^2 = \frac{\sigma_2^2(\sigma_2^2\cos^2\theta + \sigma_1^2\sin^2\theta)}{\sigma_2^2 - (\sigma_2^2-\sigma_1^2)\sin^2\varphi\sin^2\theta} \tag{34}$$

$$d_3^2 = \sigma_2^2 - (\sigma_2^2-\sigma_1^2)\sin^2\varphi\sin^2\theta \tag{35}$$

$$v_{1,2} = \frac{(\sigma_2^2-\sigma_1^2)\cos\varphi\cos\theta\sin\theta}{\sigma_2^2 - (\sigma_2^2-\sigma_1^2)\sin^2\theta} \tag{36}$$

$$v_{1,3} = \frac{-(\sigma_2^2-\sigma_1^2)\sin\varphi\cos\theta\sin\theta}{\sigma_2^2 - (\sigma_2^2-\sigma_1^2)\sin^2\varphi\sin^2\theta} \tag{37}$$

$$v_{2,3} = \frac{(\sigma_2^2-\sigma_1^2)\cos\varphi\cos\theta\sin\theta}{\sigma_2^2 - (\sigma_2^2-\sigma_1^2)\sin^2\varphi\sin^2\theta} \tag{38}$$

When checking the special cases $\sigma_1 = \sigma_2 = \sigma_3$ (isotropic Gaussian), or $\theta = k\pi$ with $k \in \mathbb{Z}$ (axis aligned Gaussian), one sees that our method of decomposition yields $V = \mathrm{Id}$ and $D = \mathrm{diag}(\sigma_1, \sigma_2, \sigma_2)$ in these cases, such that it is not necessary to treat them as exceptions.

5 Discretization & Implementation

The results from the previous sections tell us how to factorize Gaussians and we have proposed a specific factorization in Section 3.2, with properties which we expect to be useful for implementation. Before implementing the separated filter, the following issues need to be resolved.

5.1 Discrete Directional Convolution Operator

We need a discrete version of our theory. Therefore, we will from now on study discrete signals and filter masks. To clearly indicate this, we will use capital letters for those, instead of small letters in the continuous case, e.g. the Gaussian will be denoted by $G(\mathbf{x})$ instead of $g(\mathbf{x})$.

For a discrete signal on a grid, the convolution integral (11) turns into a sum:

$$(G_i *_{\mathbf{v}} F)(\mathbf{x}) = \sum_{k\in\mathbb{Z}} G_i(k)F(\mathbf{x} - k\mathbf{v}), \tag{39}$$

where the coefficients G_i are derived from the 1D-Gaussian by sampling at the grid points. With this, the discrete anisotropic Gaussian filtering (12) can be written as

$$(G * F) = G_1 *_{\mathbf{v}^1} G_2 *_{\mathbf{v}^2} \ldots G_n *_{\mathbf{v}^n} F. \tag{40}$$

5.2 Interpolation

In Equation (39), the direction vector $\mathbf{v}$ does not need to contain only integer valued entries, so $\mathbf{x} - k\mathbf{v}$ does not in general lie on the sampling grid. To obtain a value for

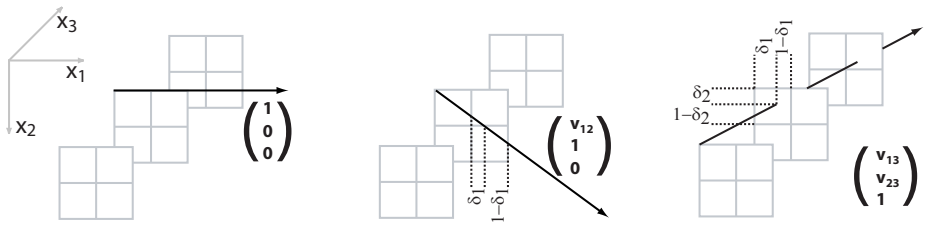

(a) (b) (c)

Figure 2: In 3D, implementing the proposed separation results in three directional convolution operations, requiring (a) no interpolation, (b) 1D, or (c) 2D interpolation.

F at this position, interpolation from neighboring sample points becomes necessary, see e.g. [21, Ch. 9].

To explain the interpolation needed when using the triangular factorization from Section 3.2, We will now study the case of $\mathbb{R}^3$. The general case can easily be extrapolated from this. The convolution is then given by

$$G * F = G_3 *_{\mathbf{v}^3} G_2 *_{\mathbf{v}^2} G_1 *_{\mathbf{v}^1} F. \tag{41}$$

Consider the first convolution step $F_2 := G_1 *_{\mathbf{v}^1} F$. Its direction is always given by $\mathbf{v}^1 = (1, 0, 0)^t$, so memory access is only necessary in unit steps along x_1. Thus, having compact memory blocks and no need for interpolation, computation of F_2 is fast and accurate.

Except when the Gaussian is axis-aligned, all subsequent directions will require interpolation orthogonal to one of the coordinate axes. We will analyze the second directional convolution, along $\mathbf{v}_2 = (v_{1,2}, 1, 0)^t$, more closely.

$$\begin{aligned} G_2 *_{\mathbf{v}^2} F_2 &= \sum_{k\in\mathbb{Z}} G_2(k) F(\mathbf{x} - k\,(v_{1,2}, 1, 0)^t) \\ &= \sum_{k\in\mathbb{Z}} G_2(k) F(x_1 - k v_{1,2}, x_2 - k, x_3), \end{aligned} \tag{42}$$

This shows that we need to interpolate along direction x_1 only. Note that this is a direct result of our choice of factorization in Section 3.2. Each following directional convolution operation will need one additional interpolation direction. In 3D, we need at most two (orthogonal) interpolation directions: let x_1, x_2, x_3 denote integer valued coordinates and $\delta_1, \delta_2 \in [0, 1[$ offsets from the voxel origins. Then, we have the following cases, as is also illustrated in Figure 2.

(a) $F(x_1, x_2, x_3)$ lies on the grid, no interpolation necessary.

(b) $F(x_1 + \delta_1, x_2, x_3)$ needs interpolation in x_1-direction.

(c) $F(x_1 + \delta_1, x_2 + \delta_2, x_3)$ needs interpolation in the x_1, x_2-plane.

The interpolations could be calculated using nearest neighbor, linear/bilinear, or higher order schemes, see e.g. [22, Ch. 8]. Performing the same analysis in $\mathbb{R}^n$, we find that up to $n-1$ interpolation directions are needed per step with interpolation in x_n never being necessary.

5.3 Finite and Infinite Impulse Response Filtering

Our proposed decomposition requires computation of n one dimensional convolutions. Here we discuss different ways for performing these operations.

Apart from filtering in Fourier space by use of the convolution theorem, finite impulse response (FIR) filtering in image space is the usual way of implementing a convolution filter. There, the convolution sum in (39) is truncated,

$$(G_i *_{\mathbf{v}} F)(\mathbf{x}) = \sum_{k=-K}^{K} G_i(k) F(\mathbf{x} - k\mathbf{v}), \tag{43}$$

where K is chosen in a way such that only terms remain in the sum where $G_i(k)$ differs significantly from 0, usually a constant multiple of the standard deviation of the Gaussian. When doing so, runtime increases with σ. This drawback can be resolved by using the infinite impulse response (IIR) implementation of Gaussian filters proposed in [15]. Therein, the authors derive a recursive filtering scheme based on a rational approximation of the Gaussian function.

The original recursive filter is defined by a pair of filters acting on a 1D-signal. To support directional filtering, we modify them to perform a 1D-convolution along a direction vector $\mathbf{v}$ within a higher dimensional grid. The resulting filter uses $\mathbf{v}$ as the unit step, analogously to Equation (43). The directional convolution operator is then decomposed into a *forward* and *backward* filter pair:

$$\begin{aligned} w(\mathbf{x}) &= BF(\mathbf{x}) + \frac{1}{b_0} \sum_{k=1}^{3} b_k w(\mathbf{x} - k\mathbf{v}) \\ (G *_{\mathbf{v}} F)(\mathbf{x}) &= Bw(\mathbf{x}) + \frac{1}{b_0} \sum_{k=1}^{3} b_k (G *_{\mathbf{v}} F)(\mathbf{x} + k\mathbf{v}) \end{aligned} \tag{44}$$

See [15] for details on the filter coefficients b_0, b_1, b_2, b_3 and B, and [23] for boundary conditions which need to be applied to correct distortions. Because only the values of the coefficients in (44) depend on σ, but their number does not, the runtime of this implementation of the Gaussian filter is independent of σ.

5.4 Implementation

There are numerous ways of implementing the discrete directional convolution operator from Eq. (39). The first, and most obvious one, is a direct implementation of the FIR filter in (43), and we will refer to it as the "naive" implementation: for each pixel or voxel in an image evaluate the convolution sum along a direction $\mathbf{v}$.

Another way of interpreting the directional convolution is to cast parallel rays in direction $\mathbf{v}$ through an image, which we call the "line buffer" implementation. Convolutions can then be computed along these lines, which is more efficient than evaluating the convolution at each image location separately. Also, the fast recursive IIR filter described in Sec. 5.3 can be applied.

Note that the convolution operator was defined at a fixed image location $\mathbf{x}$. For a general direction $\mathbf{v}$, the lines along which we want to calculate the convolutions will not lie on the sampling grid of a given image. To get an estimate of the resulting value at $\mathbf{x}$, we need to interpolate from lines around that location. In essence, this results in interpolations for both reading and writing data from the image. As above, this means that one has to perform up to $n-1$ dimensional interpolations, both for extracting values along lines and for writing values back to the image.

The third and last type of implementation that we discuss here is the "geometric" variant. We outlined in Sec. 3.4 that the matrix V in our proposed separation corresponds to a shear. Thus, the directional convolution of the whole image is readily implemented by performing a shear in the image using V^{-1}, convolving along the coordinate axes using the variance parameters derived in Sec. 4 and then performing the inverse shear using V.

Implementation of this is straight forward in 2D. In the 3D case, the following observation can lead to an efficient implementation: given the triangular matrix V with unit diagonal, the total operation can be separated into first a shear in x_1 and then a shear in x_2 direction. Shearing in x_3 is never necessary. This also implies that for this implementation, only 1D interpolations will be required in both x_1 and x_2. The convolutions along the coordinate axes can again be calculated using the recursive IIR filter. Higher dimensional data can be treated similarly.

6 Results

To show the practical use our method, we performed several experiments on speed and accuracy for two and three-dimensional data. We created our own implementations in C respectively C++, testing different methods to implement the directional convolution operators: naive, line buffer and geometric implementation, see Section 5.4.

For the recursive IIR implementation of the 1D Gaussian, we used the source code that is publicly available at the homepage of J.M. Geusebroek[1]. There, he also offers an implementation of the anisotropic 2D-Gaussian filter as it was proposed in [13]. We included this into our tests as well, because although it works similar to our line buffer method, it differs from it by integrating the interpolation into the Gaussian filtering steps.

So far, the method of choice for anisotropic Gaussian filtering is convolution in the Fourier transform (FT) domain. Therefore, we present our performance results in comparison with the speed of anisotropic Gaussian filtering based on the Fast Fourier Transform. As FFT-implementation we used the fftw v3 library[2] in single precision mode. This state-of-the-art library is highly optimized, including hand-optimized SIMD assembler code. It is widely recognized as the best implementation of the discrete FT currently available. Single precision with real input data is its fastest mode of operation.

6.1 Accuracy

One important aspect is the accuracy of our method of separation in comparison to an exact Gaussian convolution. To study this, we analyze the impulse response, which is the result of filtering a delta impulse. Impulse responses are characteristic for every linear filter, and for Gaussian filtering, they should exactly have the form of the Gaussian that is used for filtering.

In Figure 3 we give 2D-contour plots of the impulse responses in 3D, using the geometric implementation, acting on single precision floats and utilizing two different interpolation schemes. As mentioned in our geometric interpretation in Section 3.4, for a perfect Gaussian filter the depicted contours should be ellipses.

To also give an impression of the correct localization and orientation, we also plot 1D cross sections of the 3D impulse response along one coordinate axis while keeping the other two fixed. This is shown in Figure 4, once at the coordinate center, and once at a position 10 voxels away. Here, the correctly shaped Gaussians are also depicted in the plots as reference.

6.2 Speed

The main motivation for deriving a separable anisotropic Gaussian convolution filter is to achieve a faster implementation than those previously available. We therefore

[1] `http://staff.science.uva.nl/~mark/`
[2] `http://www.fftw.org`

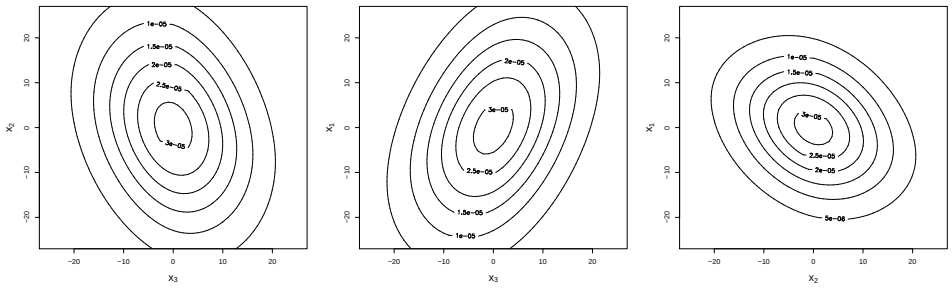

(a) Convolution using single precision floating point data and linear/bilinear interpolation

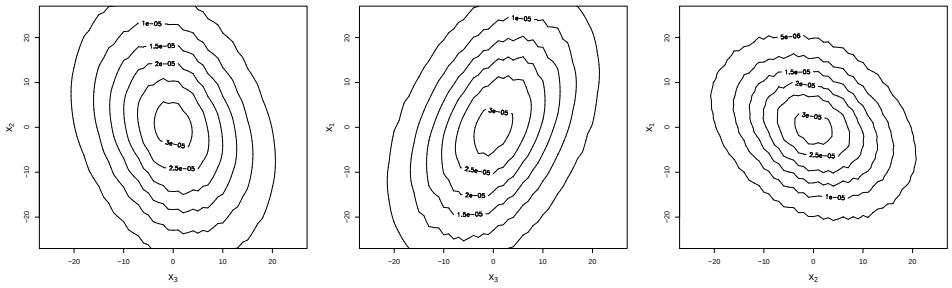

(b) Convolution using single precision floating point data and nearest neighbor interpolation

Figure 3: Orthogonal slices through the impulse response of our 3D implementation, $\theta = 30°$, $\varphi = 60°$, $\sigma_1 = 20$ and $\sigma_2 = \sigma_3 = 10$. For a perfect Gaussian, the contour lines are ellipses centered at the origin.

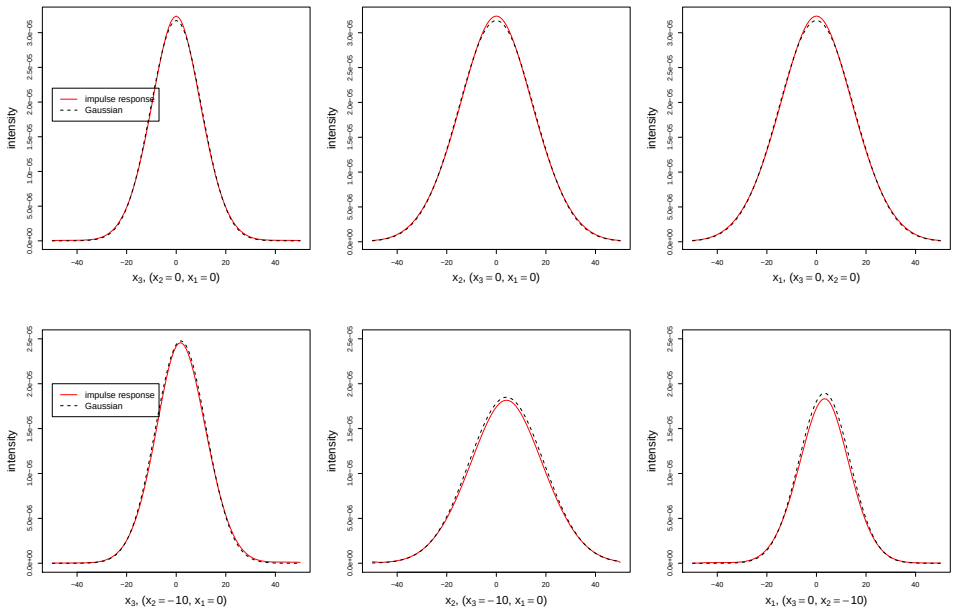

Figure 4: One-dimensional profiles across the impulse responses from Figure 3(a) against the true Gaussian function at the coordinate center (top) and shifted by 10 voxels from the center (bottom)

did experiments on the filter speed, the results of which are presented in Figure 5. It shows the absolute performance (measured as the total runtime) and the filter throughput (measured as the number of image elements processed per second) of our method compared with the FFT-based method. We also plot the speed of an isotropic filter for reference. All tests were performed using images with side lengths $N = 100, 130, \ldots, 5000$ for 2D and $N = 50, 60, \ldots, 450$ for 3D.

For each measurement 30 runs were performed and their average was used after excluding the top and bottom 10% as outliers. For the FFT runtimes, measurements contain the forward and backward transforms as well as point wise multiplication with the transformed Gaussian kernel. A full Fourier transform step for the Gaussian can be avoided by pre-computing its transformed values, and is therefore not included in the timing measurements. Overhead introduced by converting the input image from possibly integer values to a floating point representation is not included, either.

For the separated Gaussian, the time needed to apply the two or three directional convolution filters was measured, also without the possible overhead due to an initial data conversion. For the detailed plots of the runtimes the geometric implementation was used, because it turned out to be fastest in our experiments. As alternative implementations, we have also tested the line buffer and the naive method, benchmarking each for different image types (float or 8 bit data) and interpolation schemes (bilinear or nearest-neighbor).

For each image size, we calculated the relative performance of all implementations compared to the reference implementation (isotropic, float data). Their average values and standard deviation over the image sizes are presented in Table 6. The runtimes of the naive implementation depend not only on the image size but also on the variance parameters. It is therefore not possible to give representative values of an average runtime.

As a hardware platform, we used a a standard PC with 2.2 GHz Athlon64 3200+

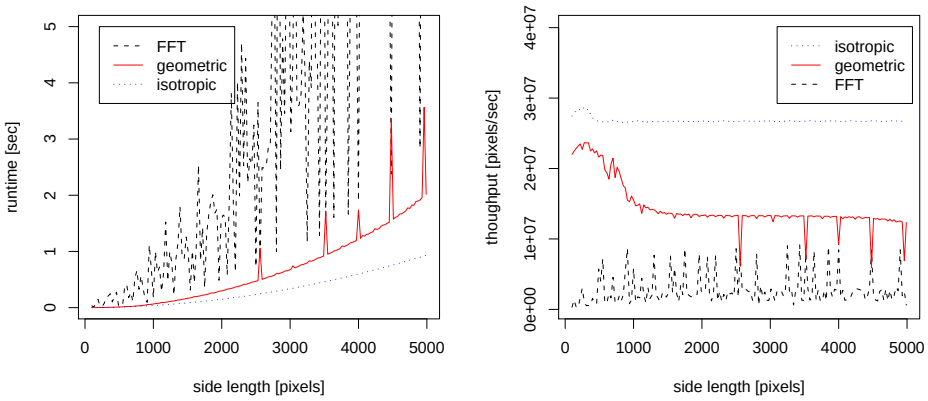

(a) 2D filtering performance: our geometric implementation vs. FFT-based convolution vs. isotropic filtering (float data)

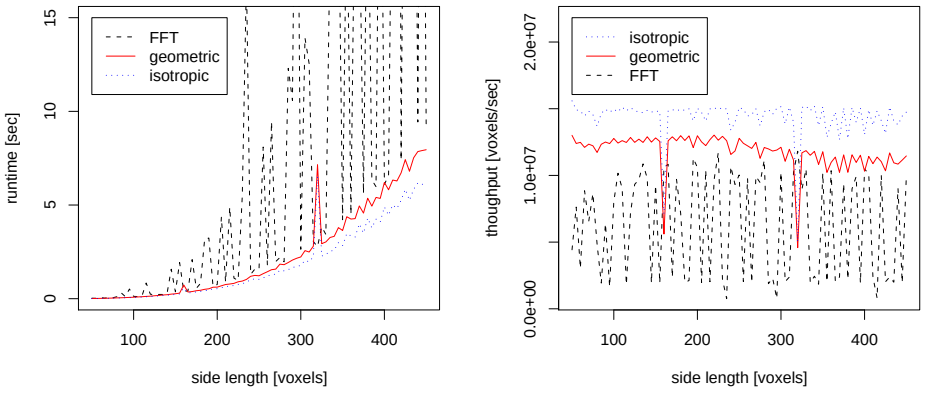

(b) 3D filtering performance: our geometric implementation vs. FFT-based convolution vs. isotropic filtering (float data)

Figure 5: Performance of different methods to calculate the anisotropic Gaussian filter: absolute speed (left) and relative throughput (right)

method	interpolation	rel. runtime float data	rel. runtime 8 bit data
isotropic		1.00	0.98 ± 0.07
geometric	nearest neighbor	1.21 ± 0.05	1.01 ± 0.07
geometric	linear	1.22 ± 0.05	1.10 ± 0.05
line buffer	nearest neighbor	2.11 ± 0.22	1.46 ± 0.16
line buffer	bilinear	3.73 ± 0.44	2.24 ± 0.27
FFT		4.30 ± 3.99 *(see text)*	
naive		depends on σ *(see text)*	

(a) 3D relative performance

method	interpolation	rel. runtime float data	rel. runtime 8 bit data
isotropic		1.00	1.59 ± 0.30
geometric	nearest neighbor	1.98 ± 0.55	1.62 ± 0.29
geometric	linear	2.01 ± 0.55	1.70 ± 0.29
line buffer	nearest neighbor	2.09 ± 0.06	2.01 ± 0.35
line buffer	linear	3.69 ± 0.15	2.89 ± 0.60
Geusebroek[13]	linear (partial)	1.29 ± 0.11	
FFT		7.69 ± 6.92 *(see text)*	
naive		depends on σ *(see text)*	

(b) 2D relative performance

Figure 6: Average performance of different implementations of the anisotropic Gaussian filter, measured in relative units. For each method, the ratio between their runtime and the runtime of the isotropic Gaussian were measure. The tables shows their mean and standard deviation over all image sizes (see text).

CPU and 1 GB of RAM, using the Intel icc 9.0 compiler under a 32 bit GNU/Linux Operating System.

7 Discussion

The results from Section 6 can be summed up into two main statements:

1. *Calculating the anisotropic Gaussian using our separation scheme is faster than the FFT-based approach, often even by a large factor.*

2. *The resulting filter is a very good approximation of the actual Gaussian.*

In the rest of this section we will discuss both statements in more detail.

7.1 Accuracy

Analyzing the accuracy, we first see in Figure 3(a) that the impulse response contours are very close to ellipses. For the linear interpolation implementation (Figure 4), the 1D-profiles almost exactly match the Gaussians, with correct width and the peaks at the correct position. This was the case for all our implementations, including those working on 8 bit data, and we therefore only present the results for the geometric IIR method, which was also used for the speed measurements. There are minor deviations in the peak height, which can mainly be explained by the interpolation error and by the fact that for simplicity, we let the IIR filter act in a wrap-around way on the image data instead of cutting the Gaussian off at the image edges. In total, the plots clearly show that our implementation indeed performs a Gaussian filtering with the correct rotational and variance parameters.

When using the simpler nearest neighbor interpolation scheme (which essentially does not perform any interpolation at all), the impulse response shows some defects, see Figure 3(b). Nevertheless, these affect the impulse response only locally. This means that the angular selectivity and support of the kernel are not compromised by implementing a lower order interpolation. While this plays less of a role on a PC platform, the fact could be important for other hardware platforms like DSPs or FPGAs.

7.2 Speed

Regarding the speed, we can see from Figure 5 that our algorithm shows a smooth runtime curve over a wide range of image sizes, also expressing itself in an almost constant number of pixels filtered per second. The small variations can be explained by caching effects, e.g. one can see that the performance is somewhat reduced if the size of an image row is a multiple of the CPU's cache line size. This could be avoided by memory prefetch or a similar mechanism.

From Table 6, we see that the speed difference between the fastest methods with linear or with nearest neighbor interpolation is small. So for most practical applications, it will not be necessary to abstain from linear interpolation. Working on 8 bit data instead of floating point numbers also can increase the speed a little, but the positive effect of the lower memory requirements is almost completely canceled out by the additional CPU cost for integer-to-floating point conversions when applying the 1D Gaussian filter. However, adapting the IIR Gaussian filter to directly work on 8 bit input data could strongly change the outcome here in favor of the data type with lower memory requirements.

The naive implementation of our separation is only of interest if both the image size and the variance parameters are small. In our tests, even then it turned out

to be slower than the other methods proposed. However, in practice it might be used in some cases there the runtime is not of importance, because of the very straight-forward way it can be implemented directly from Equation (43).

The FFT shows a completely different behavior than all other methods. In particular, its runtime varies very strongly and non monotonously with image size. This is most likely due to the fact that the FFT works with least overhead if the image size is a power of 2, but the fftw library also contains other special optimizations to reduce the overhead for certain image sizes in a similar way.

Comparing our and the FFT-based method, one can see, that the performance gains are larger in two than in three dimensions. In 2D, the non-orthogonal separable Gaussian clearly outperforms the convolution in the FT domain. In 3D, the separated filter is still faster than the FFT based implementation, but the gain is not as large, at least not for all possible image sizes.

Our explanation for this is twofold. For once, the computational complexity of the FFT-method is $O(N \log N)$, whereas the complexity of our method is $O(N)$, with N being the side length of the largest image dimension. Therefore, roughly speaking, our method has an advantage of $\log N$ over the FFT-based method, and this factor is larger in 2D data, where N can have values of several thousands, than for 3D, where N rather is in the range of a few hundreds.

The second reason is that the speed of the 3D problem is more determined by memory access than by CPU operations. Access patterns in 2D are organized in a way such that most data is already available in the CPU's cache memory. For 3D images, the access patterns are less localized, and more often data has to be fetched from the main memory. This is also backed up by the fact that the speed advantage of the isotropic Gaussian compared with our method and the FFT is larger in the 2D than in the 3D case. Also, our implementation does not include low-level optimizations like memory prefetch. Using those would surely yield in an additional speedup, as can be deduced from the results for the more optimized 2D-implementation by Geusebroek et al.

8 Applications

In this section we show some application examples of anisotropic Gauss filters, both using them as directed filters and to construct orientation space images. We have applied our method to 2D and 3D image data and to $2 + 1$D video.

8.1 Processing of Fibrous Data

Many macroscopically homogeneous materials reveal heterogeneous characteristics when examined at a microscopic scale. Quantization of such properties by means of image analysis not only in two, but also in three dimensional data, is possible using microscopic or micro-tomographic (μCT) data, respectively. Typically, binarization is a prerequisite to performing such analyses, see e.g. [24, 25]. In this setting, anisotropic filtering is a useful preprocessing tool, especially when one is dealing with images of strongly anisotropic objects such as fibers.

One such investigation of polyethylenterephthalat (PET) fibers was recently presented in [25], from where the images in Figure 7 were taken. The goal there was to optimize the material's acoustic properties. Here we present these 2D images to demonstrate the effects of anisotropic Gaussian filtering.

In the orientation space representation of the image, where one selects the parameters which maximize filter response in each pixel, the background structure was removed while keeping the fibers in the image intact. Edges are well preserved which can be attributed to the adaptive nature of this approach.

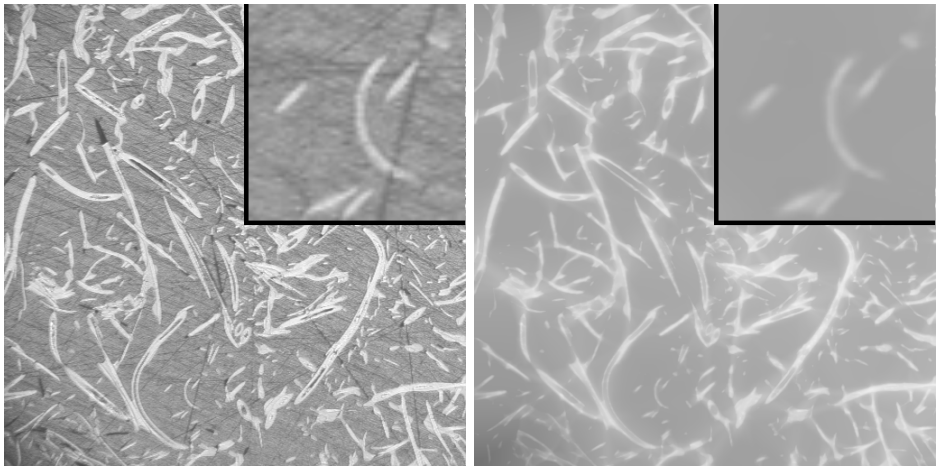

(a) original (b) orientation-space

Figure 7: Microscopic images of a polished slice of a non-woven material that is used in the automotive industry. For the orientation-space representation, all free parameters were estimated by an exhaustive search over the following ranges: $\theta = 0 \ldots 180°$ in a resolution of $10°$, $\sigma_1 = 1 \cdot \sigma_2, \ldots, 5 \cdot \sigma_2$ and $\sigma_2 = 1, \ldots, 15$.

Figure 8 shows orthogonal cross-sections of a piece of wood obtained by μCT. To reduce the level of noise, we first apply an oriented anisotropic Gauss filter in this 3D image. The rotation parameters were hand-picked to align the kernel with the fibers in this dataset. The fibrous structure is very clear in Figure 8(d). This is because the dataset has a dominant fiber direction in that slice, to which a kernel could easily be aligned. In the other slices, it becomes clear that not all fibers in the dataset are aligned with that direction, which explains the unwanted smoothing across edges in Figure 8(e) and 8(f). These defects are eliminated in the orientation space representation of the data. Structures in cross-sections orthogonal to the dominant fiber direction also become visible.

8.2 Spatiotemporal smoothing of Video Sequences

For object detection in video sequences, typically low-level image features like color and texture are used, or motion between frames is analyzed. For both, de-noising usually is the first preprocessing step, which is done individually for each frame. Afterwards, motion estimation and feature extraction are performed, again frame by frame.

An alternative unified approach relies on the covariance information between subsequent frames for smoothing. Since objects do not appear or disappear spontaneously in a video sequence, they cause dependencies between the pixel values at different time steps. This can be utilized for filtering: instead of applying a 2D-smoothing filter to each image, we make use of the correlations and apply an anisotropic 3D-smoothing filter along space and time at the same time.

Figure 8.2 illustrates this using part of the 'mobcal' video sequence provided by the Technical University of Munich[3]. It shows a moving toy train in front of a differently moving background and other objects. After filtering the sequence with a prolate 3D-Gaussian whose correlation matrix has been chosen to be aligned

[3] `ftp://ftp.ldv.e-technik.tu-muenchen.de/pub/test_sequences/1080i/`

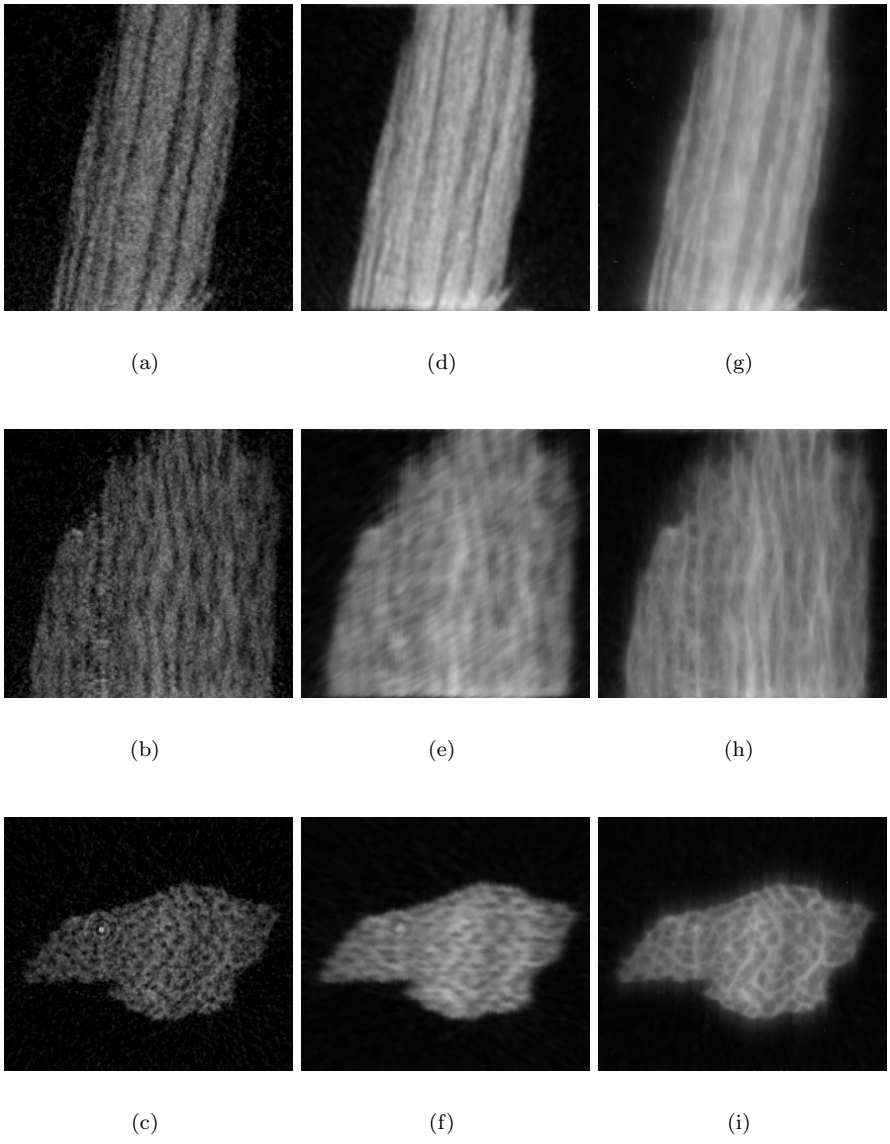

(a) (d) (g)

(b) (e) (h)

(c) (f) (i)

Figure 8: (a-c) Orthogonal cross-sections through a μCT of a piece of wood, (d-f) anisotropic filtering with parameters aligned to dominant fiber direction ($\theta = 77°$, $\varphi = 0°$, $\sigma_1 = 5$, $\sigma_2 = \sigma_3 = 1$), (g-i) orientation-space with an angular resolution of $10°$.

(a) original frame #240 (b) anisotropically filtered

Figure 9: Anisotropic filtering to selectively smoothen 2+1D video data. A strongly prolate anisotropic 3D-Gaussian is aligned with the motion of the front of the toy train. The resulting filter acts as a motion aware blurring filter, only weakly smoothing the first two cars of the train, but strongly blurring the background and other objects which show different movement patterns. Filtering the clip of 80 frames in 1920×1080 resolution takes less than 1 minute (20 seconds per color channel) on a 2GHz PC.

to the train motion, we can see that the image is blurred where the scene motion does not coincide with the train motion, while on the front of the train itself, the Gaussian mainly acts a de-noising filter, without the strong blurring effect.

9 Conclusion

We have presented a geometrically motivated new method for separating the anisotropic Gaussian filter, i.e. for decomposing its n-dimensional convolution integral into a sequence of n one-dimensional ones along arbitrary convolution axes in $\mathbb{R}^n$. From a mathematical analysis we were able to show that our method using the Triangular Factorization of Cholesky Type is optimal with regard to the number of necessary interpolation operations and memory accesses. The theory also acts as a generalization of the non-orthogonal separation scheme in $\mathbb{R}^2$ by Geusebroek et al. [14].

Since our algorithm works solely in the image domain, it is very flexible in implementation and allows to incorporate different interpolation schemes and methods to calculate the one-dimensional Gaussian (FIR, IIR). Our analysis showed that in any of these implementations, the method acts as a high accuracy Gaussian filter. Due to its structure, our filter can easily be applied locally, enabling it, for example, to cope with missing data.

The main advantage of our separation is that it is very fast. Already our plain C implementation outperforms the usual FFT-based method which makes heavy use of SIMD-assembler code. As a future improvement, we are planning to incorporate analogous optimizations into our implementation as well. This will include a version of the Gaussian IIR filter that can work on 8 bit image data without a need for integer-to-float conversion. The resulting source code will be provided for public download.

Application examples of anisotropic Gauss filters were shown to put our method into a larger context. Even though the focus of the present work was to develop a sound mathematical basis and an optimal solution for an open problem, we were able to demonstrate the usefulness of the filter for very different tasks in image processing.

One problem of our non-orthogonal separation is that the calculation of Gaussian

derivative filters is less straightforward. Because our directions of convolution do not coincide with the Gaussian's main axes, it is not possible to just convolve with a derived one-dimensional convolution kernel, as this is the case for isotropic Gaussians. The same phenomenon already exists in 2D, where the authors of [13] suggest to use rotated finite differences for calculating the derivatives. The necessary linear combinations of the filtered samples can be interwoven into the separated convolution steps themselves.

To improve the filtering method itself, it might be useful to look for even better (faster, more accurate) separations by allowing other functions than Gaussians as one-dimensional convolution kernels. The first candidates that come to mind would be of Gaussian form, but without a normalization constraint. This corresponds to transformation matrices V that are not of unit diagonal anymore. The result would be a higher number of possible choices for the separation matrices, in some cases allowing shorter direction vectors for the 1D convolutions, and thus more accurate interpolation and better locality of memory accesses. We plan to study this in a subsequent publication.

References

[1] G.-Z. Yang, P. Burger, D. N. Firmin, and S. R. Underwood, "Structure adaptive anisotropic image filtering." *Image Vision Comput.*, vol. 14, no. 2, pp. 135–145, 1996.

[2] M. Lynch, K. Robinson, O. Ghita, and P. Whelan, "A performance characterisation in advanced data smoothing techniques," in *Proc. Irish Machine Vision and Image Processing Conference (IMVIP)*, 2004.

[3] J. Wang, B. Thiesson, Y. Xu, and M. Cohen, "Image and video segmentation by anisotropic kernel mean shift." in *ECCV (2)*, ser. Lecture Notes in Computer Science, T. Pajdla and J. Matas, Eds., vol. 3022. Springer, 2004, pp. 238–249.

[4] K. Okada, D. Comaniciu, N. Dalal, and A. Krishnan, "A robust algorithm for characterizing anisotropic local structures," in *European Conference on Computer Vision*, J. M. Tomás Pajdla, Ed., vol. 1, ECCV. Springer-Verlag Heidelberg, apr 2004, pp. 549 – 561.

[5] K. Okada, D. Comaniciu, and A. Krishnan, "Scale selection for anisotropic scale-space: Application to volumetric tumor characterization," in *Proc. IEEE Conf. Computer Vision and Pattern Recognition (CVPR)*, 2004.

[6] R. Manmatha and N. Srimal, "Scale space technique for word segmentation in handwritten documents." in *Scale-Space*, ser. Lecture Notes in Computer Science, M. Nielsen, P. Johansen, O. F. Olsen, and J. Weickert, Eds., vol. 1682. Springer, 1999, pp. 22–33.

[7] V. Lakshmanan, "A separable filter for directional smoothing," *IEEE Transactions on Geoscience and Remote Sensing Letters*, vol. 1, no. 3, pp. 192–195, 2004.

[8] F. G. A. Faas and L. J. van Vliet, "3D-orientation space; filters and sampling." in *SCIA*, ser. Lecture Notes in Computer Science, J. Bigün and T. Gustavsson, Eds., vol. 2749. Springer, 2003, pp. 36–42.

[9] T. Lindeberg, *Scale-Space Theory in Computer Vision.* Norwell, MA, USA: Kluwer Academic Publishers, 1994.

[10] J. Loviscach, "Motion blur for textures by means of anisotropic filtering," in *Rendering Techniques 2005 (Eurographic Symposium on Rendering)*, 2005, pp. 105–110.

[11] W. T. Freeman and E. H. Adelson, "The design and use of steerable filters," *IEEE Trans. Pattern Analysis and Machine Intelligence*, vol. 13, no. 9, pp. 891–906, 1991.

[12] P. Perona, "Steerable-scalable kernels for edge detection and junction analysis," *Image Vision Comput.*, vol. 10, no. 10, pp. 663–672, 1992.

[13] J.-M. Geusebroek, A. W. M. Smeulders, and J. van de Weijer, "Fast anisotropic gauss filtering," in *ECCV '02: Proceedings of the 7th European Conference on Computer Vision-Part I.* London, UK: Springer-Verlag, 2002, pp. 99–112.

[14] ——, "Fast anisotropic gauss filtering," *IEEE Trans. Image Proc.*, vol. 23, no. 8, pp. 938–943, 2003.

[15] I. Young and L. van Vliet, "Recursive implementation of the gaussian filter," *Signal Processing*, vol. 44, pp. 139–151, 1995.

[16] O. Wirjadi and T. Breuel, "Approximate separable 3D anisotropic gauss filter," in *Proc. IEEE International Conference on Image Processing (ICIP 2005)*, 2005.

[17] R. O. Duda, P. E. Hart, and D. G. Stork, *Pattern Classification*, 2nd ed. Wiley-Interscience, 2000.

[18] G. Golub and C. V. Loan, *Matrix Computations*, 3rd ed. Johns Hopkins University Press, 1996.

[19] G. Strang, *Introduction to Applied Mathematics.* Wellesley-Cambridge Press, 1986.

[20] E. Weisstein, *CRC Concise Encyclopedia of Mathematics*, 2nd ed. Chapman & Hall/CRC, 2002.

[21] J. Proakis and D. Manolakis, *Digital Signal Processing: Principles, Algorithms, and Applications*, 3rd ed. Upper Saddle River, NJ, USA: Prentice Hall, 1996.

[22] J. Lim, *Two-Dimensional Signal and Image Processing.* Prentice-Hall, 1990.

[23] B. Triggs and M. Sdika, "Boundary conditions for young - van vliet recursive filtering," 2005, to appear in IEEE Transactions on Signal Processing.

[24] C. Lang, J. Ohser, and R. Hilfer, "On the analysis of spatial binary images," *Journal of Microscopy*, vol. 203, pp. 303–313, 2001.

[25] K. Schladitz, S. Peters, D. Reinel-Bitzer, A. Wiegmann, and J. Ohser, "Design of acoustic trim based on geometric modeling and flow simulation for non-woven," Fraunhofer ITWM, Kaiserslautern, Report 72, 2005. [Online]. Available: http://www.itwm.fraunhofer.de/zentral/download/berichte/bericht72.pdf

Published reports of the Fraunhofer ITWM

The PDF-files of the following reports are available under:
www.itwm.fraunhofer.de/de/zentral__berichte/berichte

1. D. Hietel, K. Steiner, J. Struckmeier

A Finite - Volume Particle Method for Compressible Flows

We derive a new class of particle methods for conservation laws, which are based on numerical flux functions to model the interactions between moving particles. The derivation is similar to that of classical Finite-Volume methods; except that the fixed grid structure in the Finite-Volume method is substituted by so-called mass packets of particles. We give some numerical results on a shock wave solution for Burgers equation as well as the well-known one-dimensional shock tube problem.
(19 pages, 1998)

2. M. Feldmann, S. Seibold

Damage Diagnosis of Rotors: Application of Hilbert Transform and Multi-Hypothesis Testing

In this paper, a combined approach to damage diagnosis of rotors is proposed. The intention is to employ signal-based as well as model-based procedures for an improved detection of size and location of the damage. In a first step, Hilbert transform signal processing techniques allow for a computation of the signal envelope and the instantaneous frequency, so that various types of non-linearities due to a damage may be identified and classified based on measured response data. In a second step, a multi-hypothesis bank of Kalman Filters is employed for the detection of the size and location of the damage based on the information of the type of damage provided by the results of the Hilbert transform.
Keywords: Hilbert transform, damage diagnosis, Kalman filtering, non-linear dynamics
(23 pages, 1998)

3. Y. Ben-Haim, S. Seibold

Robust Reliability of Diagnostic Multi-Hypothesis Algorithms: Application to Rotating Machinery

Damage diagnosis based on a bank of Kalman filters, each one conditioned on a specific hypothesized system condition, is a well recognized and powerful diagnostic tool. This multi-hypothesis approach can be applied to a wide range of damage conditions. In this paper, we will focus on the diagnosis of cracks in rotating machinery. The question we address is: how to optimize the multi-hypothesis algorithm with respect to the uncertainty of the spatial form and location of cracks and their resulting dynamic effects. First, we formulate a measure of the reliability of the diagnostic algorithm, and then we discuss modifications of the diagnostic algorithm for the maximization of the reliability. The reliability of a diagnostic algorithm is measured by the amount of uncertainty consistent with no-failure of the diagnosis. Uncertainty is quantitatively represented with convex models.
Keywords: Robust reliability, convex models, Kalman filtering, multi-hypothesis diagnosis, rotating machinery, crack diagnosis
(24 pages, 1998)

4. F.-Th. Lentes, N. Siedow

Three-dimensional Radiative Heat Transfer in Glass Cooling Processes

For the numerical simulation of 3D radiative heat transfer in glasses and glass melts, practically applicable mathematical methods are needed to handle such problems optimal using workstation class computers. Since the exact solution would require super-computer capabilities we concentrate on approximate solutions with a high degree of accuracy. The following approaches are studied: 3D diffusion approximations and 3D ray-tracing methods.
(23 pages, 1998)

5. A. Klar, R. Wegener

A hierarchy of models for multilane vehicular traffic
Part I: Modeling

In the present paper multilane models for vehicular traffic are considered. A microscopic multilane model based on reaction thresholds is developed. Based on this model an Enskog like kinetic model is developed. In particular, care is taken to incorporate the correlations between the vehicles. From the kinetic model a fluid dynamic model is derived. The macroscopic coefficients are deduced from the underlying kinetic model. Numerical simulations are presented for all three levels of description in [10]. Moreover, a comparison of the results is given there.
(23 pages, 1998)

Part II: Numerical and stochastic investigations

In this paper the work presented in [6] is continued. The present paper contains detailed numerical investigations of the models developed there. A numerical method to treat the kinetic equations obtained in [6] are presented and results of the simulations are shown. Moreover, the stochastic correlation model used in [6] is described and investigated in more detail.
(17 pages, 1998)

6. A. Klar, N. Siedow

Boundary Layers and Domain Decomposition for Radiative Heat Transfer and Diffusion Equations: Applications to Glass Manufacturing Processes

In this paper domain decomposition methods for radiative transfer problems including conductive heat transfer are treated. The paper focuses on semi-transparent materials, like glass, and the associated conditions at the interface between the materials. Using asymptotic analysis we derive conditions for the coupling of the radiative transfer equations and a diffusion approximation. Several test cases are treated and a problem appearing in glass manufacturing processes is computed. The results clearly show the advantages of a domain decomposition approach. Accuracy equivalent to the solution of the global radiative transfer solution is achieved, whereas computation time is strongly reduced.
(24 pages, 1998)

7. I. Choquet

Heterogeneous catalysis modelling and numerical simulation in rarified gas flows
Part I: Coverage locally at equilibrium

A new approach is proposed to model and simulate numerically heterogeneous catalysis in rarefied gas flows. It is developed to satisfy all together the following points:
1) describe the gas phase at the microscopic scale, as required in rarefied flows,
2) describe the wall at the macroscopic scale, to avoid prohibitive computational costs and consider not only crystalline but also amorphous surfaces,
3) reproduce on average macroscopic laws correlated with experimental results and
4) derive analytic models in a systematic and exact way.
The problem is stated in the general framework of a non static flow in the vicinity of a catalytic and non porous surface (without aging). It is shown that the exact and systematic resolution method based on the Laplace transform, introduced previously by the author to model collisions in the gas phase, can be extended to the present problem. The proposed approach is applied to the modelling of the EleyRideal and LangmuirHinshelwood recombinations, assuming that the coverage is locally at equilibrium. The models are developed considering one atomic species and extended to the general case of several atomic species. Numerical calculations show that the models derived in this way reproduce with accuracy behaviors observed experimentally.
(24 pages, 1998)

8. J. Ohser, B. Steinbach, C. Lang

Efficient Texture Analysis of Binary Images

A new method of determining some characteristics of binary images is proposed based on a special linear filtering. This technique enables the estimation of the area fraction, the specific line length, and the specific integral of curvature. Furthermore, the specific length of the total projection is obtained, which gives detailed information about the texture of the image. The influence of lateral and directional resolution depending on the size of the applied filter mask is discussed in detail. The technique includes a method of increasing directional resolution for texture analysis while keeping lateral resolution as high as possible.
(17 pages, 1998)

9. J. Orlik

Homogenization for viscoelasticity of the integral type with aging and shrinkage

A multiphase composite with periodic distributed inclusions with a smooth boundary is considered in this contribution. The composite component materials are supposed to be linear viscoelastic and aging (of the nonconvolution integral type, for which the Laplace transform with respect to time is not effectively applicable) and are subjected to isotropic shrinkage. The free shrinkage deformation can be considered as a fictitious temperature deformation in the behavior law. The procedure presented in this paper proposes a way to determine average (effective homogenized) viscoelastic and shrinkage (temperature) composite properties and the homogenized stressfield from known properties of the components. This is done by the extension of the asymptotic homogenization technique known for pure elastic nonhomogeneous bodies to the nonhomogeneous thermoviscoelasticity of the integral nonconvolution type. Up to now, the homogenization theory has not covered viscoelasticity of the integral type. SanchezPalencia (1980), Francfort & Suquet (1987) (see [2], [9]) have considered homogenization for viscoelasticity of the differential form and only up to the first derivative order. The integralmodeled viscoelasticity is more general then the differential one and includes almost all known differential models. The homogenization procedure is based on the construction of an asymptotic solution with respect to a period of the composite structure. This reduces the original problem to some auxiliary boundary value problems of elasticity and viscoelasticity on the unit periodic cell, of the same type as the original non-homogeneous problem. The existence and uniqueness results for such problems were obtained for kernels satisfying some constrain conditions. This is done by the extension of the Volterra integral operator theory to the Volterra operators with respect to the time, whose 1 kernels are space linear operators for any fixed time variables. Some ideas of such approach were proposed in [11] and [12], where the Volterra operators with kernels depending additionally on parameter were considered. This manuscript delivers results of the same nature for the case of the spaceoperator kernels.
(20 pages, 1998)

10. J. Mohring

Helmholtz Resonators with Large Aperture

The lowest resonant frequency of a cavity resonator is usually approximated by the classical Helmholtz formula. However, if the opening is rather large and the front wall is narrow this formula is no longer valid. Here we present a correction which is of third order in the ratio of the diameters of aperture and cavity. In addition to the high accuracy it allows to estimate the damping due to radiation. The result is found by applying the method of matched asymptotic expansions. The correction contains form factors describing the shapes of opening and cavity. They are computed for a number of standard geometries. Results are compared with numerical computations.
(21 pages, 1998)

11. H. W. Hamacher, A. Schöbel

On Center Cycles in Grid Graphs

Finding "good" cycles in graphs is a problem of great interest in graph theory as well as in locational analysis. We show that the center and median problems are NP hard in general graphs. This result holds both for the variable cardinality case (i.e. all cycles of the graph are considered) and the fixed cardinality case (i.e. only cycles with a given cardinality p are feasible). Hence it is of interest to investigate special cases where the problem is solvable in polynomial time. In grid graphs, the variable cardinality case is, for instance, trivially solvable if the shape of the cycle can be chosen freely.
If the shape is fixed to be a rectangle one can analyze rectangles in grid graphs with, in sequence, fixed dimension, fixed cardinality, and variable cardinality. In all cases a complete characterization of the optimal cycles and closed form expressions of the optimal objective values are given, yielding polynomial time algorithms for all cases of center rectangle problems.
Finally, it is shown that center cycles can be chosen as rectangles for small cardinalities such that the center cycle problem in grid graphs is in these cases completely solved.
(15 pages, 1998)

12. H. W. Hamacher, K.-H. Küfer

Inverse radiation therapy planning - a multiple objective optimisation approach

For some decades radiation therapy has been proved successful in cancer treatment. It is the major task of clinical radiation treatment planning to realize on the one hand a high level dose of radiation in the cancer tissue in order to obtain maximum tumor control. On the other hand it is obvious that it is absolutely necessary to keep in the tissue outside the tumor, particularly in organs at risk, the unavoidable radiation as low as possible.
No doubt, these two objectives of treatment planning - high level dose in the tumor, low radiation outside the tumor - have a basically contradictory nature. Therefore, it is no surprise that inverse mathematical models with dose distribution bounds tend to be infeasible in most cases. Thus, there is need for approximations compromising between overdosing the organs at risk and underdosing the target volume.
Differing from the currently used time consuming iterative approach, which measures deviation from an ideal (non-achievable) treatment plan using recursively trial-and-error weights for the organs of interest, we go a new way trying to avoid a priori weight choices and consider the treatment planning problem as a multiple objective linear programming problem: with each organ of interest, target tissue as well as organs at risk, we associate an objective function measuring the maximal deviation from the prescribed doses.
We build up a data base of relatively few efficient solutions representing and approximating the variety of Pareto solutions of the multiple objective linear programming problem. This data base can be easily scanned by physicians looking for an adequate treatment plan with the aid of an appropriate online tool.
(14 pages, 1999)

13. C. Lang, J. Ohser, R. Hilfer

On the Analysis of Spatial Binary Images

This paper deals with the characterization of microscopically heterogeneous, but macroscopically homogeneous spatial structures. A new method is presented which is strictly based on integral-geometric formulae such as Crofton's intersection formulae and Hadwiger's recursive definition of the Euler number. The corresponding algorithms have clear advantages over other techniques. As an example of application we consider the analysis of spatial digital images produced by means of Computer Assisted Tomography.
(20 pages, 1999)

14. M. Junk

On the Construction of Discrete Equilibrium Distributions for Kinetic Schemes

A general approach to the construction of discrete equilibrium distributions is presented. Such distribution functions can be used to set up Kinetic Schemes as well as Lattice Boltzmann methods. The general principles are also applied to the construction of Chapman Enskog distributions which are used in Kinetic Schemes for compressible Navier-Stokes equations.
(24 pages, 1999)

15. M. Junk, S. V. Raghurame Rao

A new discrete velocity method for Navier-Stokes equations

The relation between the Lattice Boltzmann Method, which has recently become popular, and the Kinetic Schemes, which are routinely used in Computational Fluid Dynamics, is explored. A new discrete velocity model for the numerical solution of Navier-Stokes equations for incompressible fluid flow is presented by combining both the approaches. The new scheme can be interpreted as a pseudo-compressibility method and, for a particular choice of parameters, this interpretation carries over to the Lattice Boltzmann Method.
(20 pages, 1999)

16. H. Neunzert

Mathematics as a Key to Key Technologies

The main part of this paper will consist of examples, how mathematics really helps to solve industrial problems; these examples are taken from our Institute for Industrial Mathematics, from research in the Technomathematics group at my university, but also from ECMI groups and a company called TecMath, which originated 10 years ago from my university group and has already a very successful history.
(39 pages (4 PDF-Files), 1999)

17. J. Ohser, K. Sandau

Considerations about the Estimation of the Size Distribution in Wicksell's Corpuscle Problem

Wicksell's corpuscle problem deals with the estimation of the size distribution of a population of particles, all having the same shape, using a lower dimensional sampling probe. This problem was originary formulated for particle systems occurring in life sciences but its solution is of actual and increasing interest in materials science. From a mathematical point of view, Wicksell's problem is an inverse problem where the interesting size distribution is the unknown part of a Volterra equation. The problem is often regarded ill-posed, because the structure of the integrand implies unstable numerical solutions. The accuracy of the numerical solutions is considered here using the condition number, which allows to compare different numerical methods with different (equidistant) class sizes and which indicates, as one result, that a finite section thickness of the probe reduces the numerical problems. Furthermore, the relative error of estimation is computed which can be split into two parts. One part consists of the relative discretization error that increases for increasing class size, and the second part is related to the relative statistical error which increases with decreasing class size. For both parts, upper bounds can be given and the sum of them indicates an optimal class width depending on some specific constants.
(18 pages, 1999)

18. E. Carrizosa, H. W. Hamacher, R. Klein, S. Nickel

Solving nonconvex planar location problems by finite dominating sets

It is well-known that some of the classical location problems with polyhedral gauges can be solved in polynomial time by finding a finite dominating set, i. e. a finite set of candidates guaranteed to contain at least one optimal location.
In this paper it is first established that this result holds for a much larger class of problems than currently considered in the literature. The model for which this result can be proven includes, for instance, location problems with attraction and repulsion, and location-allocation problems.
Next, it is shown that the approximation of general gauges by polyhedral ones in the objective function of our general model can be analyzed with regard to the subsequent error in the optimal objective value. For the approximation problem two different approaches are described, the sandwich procedure and the greedy algorithm. Both of these approaches lead - for fixed epsilon - to polynomial approximation algorithms with accuracy epsilon for solving the general model considered in this paper.
Keywords: Continuous Location, Polyhedral Gauges, Finite Dominating Sets, Approximation, Sandwich Algorithm, Greedy Algorithm
(19 pages, 2000)

19. A. Becker

A Review on Image Distortion Measures

Within this paper we review image distortion measures. A distortion measure is a criterion that assigns a "quality number" to an image. We distinguish between mathematical distortion measures and those distortion measures in-cooperating a priori knowledge about the imaging devices (e. g. satellite images), image processing algorithms or the human physiology. We will consider representative examples of different kinds of distortion measures and are going to discuss them.
Keywords: Distortion measure, human visual system
(26 pages, 2000)

20. H. W. Hamacher, M. Labbé, S. Nickel, T. Sonneborn

Polyhedral Properties of the Uncapacitated Multiple Allocation Hub Location Problem

We examine the feasibility polyhedron of the uncapacitated hub location problem (UHL) with multiple allocation, which has applications in the fields of air passenger and cargo transportation, telecommunication and postal delivery services. In particular we determine the dimension and derive some classes of facets of this polyhedron. We develop some general rules about lifting facets from the uncapacitated facility location (UFL) for UHL and projecting facets from UHL to UFL. By applying these rules we get a new class of facets for UHL which dominates the inequalities in the original formulation. Thus we get a new formulation of UHL whose constraints are all facet–defining. We show its superior computational performance by benchmarking it on a well known data set.
Keywords: integer programming, hub location, facility location, valid inequalities, facets, branch and cut
(21 pages, 2000)

21. H. W. Hamacher, A. Schöbel

Design of Zone Tariff Systems in Public Transportation

Given a public transportation system represented by its stops and direct connections between stops, we consider two problems dealing with the prices for the customers: The fare problem in which subsets of stops are already aggregated to zones and "good" tariffs have to be found in the existing zone system. Closed form solutions for the fare problem are presented for three objective functions. In the zone problem the design of the zones is part of the problem. This problem is NP hard and we therefore propose three heuristics which prove to be very successful in the redesign of one of Germany's transportation systems.
(30 pages, 2001)

22. D. Hietel, M. Junk, R. Keck, D. Teleaga

The Finite-Volume-Particle Method for Conservation Laws

In the Finite-Volume-Particle Method (FVPM), the weak formulation of a hyperbolic conservation law is discretized by restricting it to a discrete set of test functions. In contrast to the usual Finite-Volume approach, the test functions are not taken as characteristic functions of the control volumes in a spatial grid, but are chosen from a partition of unity with smooth and overlapping partition functions (the particles), which can even move along pre- scribed velocity fields. The information exchange between particles is based on standard numerical flux functions. Geometrical information, similar to the surface area of the cell faces in the Finite-Volume Method and the corresponding normal directions are given as integral quantities of the partition functions. After a brief derivation of the Finite-Volume-Particle Method, this work focuses on the role of the geometric coefficients in the scheme.
(16 pages, 2001)

23. T. Bender, H. Hennes, J. Kalcsics, M. T. Melo, S. Nickel

Location Software and Interface with GIS and Supply Chain Management

The objective of this paper is to bridge the gap between location theory and practice. To meet this objective focus is given to the development of software capable of addressing the different needs of a wide group of users. There is a very active community on location theory encompassing many research fields such as operations research, computer science, mathematics, engineering, geography, economics and marketing. As a result, people working on facility location problems have a very diverse background and also different needs regarding the software to solve these problems. For those interested in non-commercial applications (e. g. students and researchers), the library of location algorithms (LoLA can be of considerable assistance. LoLA contains a collection of efficient algorithms for solving planar, network and discrete facility location problems. In this paper, a detailed description of the functionality of LoLA is presented. In the fields of geography and marketing, for instance, solving facility location problems requires using large amounts of demographic data. Hence, members of these groups (e. g. urban planners and sales managers) often work with geographical information too s. To address the specific needs of these users, LoLA was inked to a geographical information system (GIS) and the details of the combined functionality are described in the paper. Finally, there is a wide group of practitioners who need to solve large problems and require special purpose software with a good data interface. Many of such users can be found, for example, in the area of supply chain management (SCM). Logistics activities involved in strategic SCM include, among others, facility location planning. In this paper, the development of a commercial location software tool is also described. The too is embedded in the Advanced Planner and Optimizer SCM software developed by SAP AG, Walldorf, Germany. The paper ends with some conclusions and an outlook to future activities.

Keywords: facility location, software development, geographical information systems, supply chain management

(48 pages, 2001)

24. H. W. Hamacher, S. A. Tjandra

Mathematical Modelling of Evacuation Problems: A State of Art

This paper details models and algorithms which can be applied to evacuation problems. While it concentrates on building evacuation many of the results are applicable also to regional evacuation. All models consider the time as main parameter, where the travel time between components of the building is part of the input and the overall evacuation time is the output. The paper distinguishes between macroscopic and microscopic evacuation models both of which are able to capture the evacuees' movement over time.

Macroscopic models are mainly used to produce good lower bounds for the evacuation time and do not consider any individual behavior during the emergency situation. These bounds can be used to analyze existing buildings or help in the design phase of planning a building. Macroscopic approaches which are based on dynamic network flow models (minimum cost dynamic flow, maximum dynamic flow, universal maximum flow, quickest path and quickest flow) are described. A special feature of the presented approach is the fact, that travel times of evacuees are not restricted to be constant, but may be density dependent. Using multicriteria optimization priority regions and blockage due to fire or smoke may be considered. It is shown how the modelling can be done using time parameter either as discrete or continuous parameter.

Microscopic models are able to model the individual evacuee's characteristics and the interaction among evacuees which influence their movement. Due to the corresponding huge amount of data one uses simulation approaches. Some probabilistic laws for individual evacuee's movement are presented. Moreover ideas to model the evacuee's movement using cellular automata (CA) and resulting software are presented.

In this paper we will focus on macroscopic models and only summarize some of the results of the microscopic approach. While most of the results are applicable to general evacuation situations, we concentrate on building evacuation.

(44 pages, 2001)

25. J. Kuhnert, S. Tiwari

Grid free method for solving the Poisson equation

A Grid free method for solving the Poisson equation is presented. This is an iterative method. The method is based on the weighted least squares approximation in which the Poisson equation is enforced to be satisfied in every iterations. The boundary conditions can also be enforced in the iteration process. This is a local approximation procedure. The Dirichlet, Neumann and mixed boundary value problems on a unit square are presented and the analytical solutions are compared with the exact solutions. Both solutions matched perfectly.

Keywords: Poisson equation, Least squares method, Grid free method

(19 pages, 2001)

26. T. Götz, H. Rave, D. Reinel-Bitzer, K. Steiner, H. Tiemeier

Simulation of the fiber spinning process

To simulate the influence of process parameters to the melt spinning process a fiber model is used and coupled with CFD calculations of the quench air flow. In the fiber model energy, momentum and mass balance are solved for the polymer mass flow. To calculate the quench air the Lattice Boltzmann method is used. Simulations and experiments for different process parameters and hole configurations are compared and show a good agreement.

Keywords: Melt spinning, fiber model, Lattice Boltzmann, CFD

(19 pages, 2001)

27. A. Zemitis

On interaction of a liquid film with an obstacle

In this paper mathematical models for liquid films generated by impinging jets are discussed. Attention is stressed to the interaction of the liquid film with some obstacle. S. G. Taylor [Proc. R. Soc. London Ser. A 253, 313 (1959)] found that the liquid film generated by impinging jets is very sensitive to properties of the wire which was used as an obstacle. The aim of this presentation is to propose a modification of the Taylor's model, which allows to simulate the film shape in cases, when the angle between jets is different from 180°. Numerical results obtained by discussed models give two different shapes of the liquid film similar as in Taylors experiments. These two shapes depend on the regime: either droplets are produced close to the obstacle or not. The difference between two regimes becomes larger if the angle between jets decreases. Existence of such two regimes can be very essential for some applications of impinging jets, if the generated liquid film can have a contact with obstacles.

Keywords: impinging jets, liquid film, models, numerical solution, shape

(22 pages, 2001)

28. I. Ginzburg, K. Steiner

Free surface lattice-Boltzmann method to model the filling of expanding cavities by Bingham Fluids

The filling process of viscoplastic metal alloys and plastics in expanding cavities is modelled using the lattice Boltzmann method in two and three dimensions. These models combine the regularized Bingham model for viscoplastic with a free-interface algorithm. The latter is based on a modified immiscible lattice Boltzmann model in which one species is the fluid and the other one is considered as vacuum. The boundary conditions at the curved liquid-vacuum interface are met without any geometrical front reconstruction from a first-order Chapman-Enskog expansion. The numerical results obtained with these models are found in good agreement with available theoretical and numerical analysis.

Keywords: Generalized LBE, free-surface phenomena, interface boundary conditions, filling processes, Bingham viscoplastic model, regularized models

(22 pages, 2001)

29. H. Neunzert

»Denn nichts ist für den Menschen als Menschen etwas wert, was er nicht mit Leidenschaft tun kann«
Vortrag anlässlich der Verleihung des Akademiepreises des Landes Rheinland-Pfalz am 21.11.2001

Was macht einen guten Hochschullehrer aus? Auf diese Frage gibt es sicher viele verschiedene, fachbezogene Antworten, aber auch ein paar allgemeine Gesichtspunkte: es bedarf der »Leidenschaft« für die Forschung (Max Weber), aus der dann auch die Begeisterung für die Lehre erwächst. Forschung und Lehre gehören zusammen, um die Wissenschaft als lebendiges Tun vermitteln zu können. Der Vortrag gibt Beispiele dafür, wie in angewandter Mathematik Forschungsaufgaben aus praktischen Alltagsproblemstellungen erwachsen, die in die Lehre auf verschiedenen Stufen (Gymnasium bis Graduiertenkolleg) einfließen; er leitet damit auch zu einem aktuellen Forschungsgebiet, der Mehrskalenanalyse mit ihren vielfältigen Anwendungen in Bildverarbeitung, Materialentwicklung und Strömungsmechanik über, was aber nur kurz gestreift wird. Mathematik erscheint hier als eine moderne Schlüsseltechnologie, die aber auch enge Beziehungen zu den Geistes- und Sozialwissenschaften hat.

Keywords: Lehre, Forschung, angewandte Mathematik, Mehrskalenanalyse, Strömungsmechanik

(18 pages, 2001)

30. J. Kuhnert, S. Tiwari

Finite pointset method based on the projection method for simulations of the incompressible Navier-Stokes equations

A Lagrangian particle scheme is applied to the projection method for the incompressible Navier-Stokes equations. The approximation of spatial derivatives is obtained by the weighted least squares method. The pressure Poisson equation is solved by a local iterative procedure with the help of the least squares method. Numerical tests are performed for two dimensional cases. The Couette flow, Poiseuelle flow, decaying shear flow and the driven cavity flow are presented. The numerical solutions are obtained for stationary as well as instationary cases and are compared with the analytical solutions for channel flows. Finally, the driven cavity in a unit square is considered and the stationary solution obtained from this scheme is compared with that from the finite element method.

Keywords: Incompressible Navier-Stokes equations, Meshfree method, Projection method, Particle scheme, Least squares approximation

AMS subject classification: 76D05, 76M28

(25 pages, 2001)

31. R. Korn, M. Krekel

Optimal Portfolios with Fixed Consumption or Income Streams

We consider some portfolio optimisation problems where either the investor has a desire for an a priori specified consumption stream or/and follows a deterministic pay in scheme while also trying to maximize expected utility from final wealth. We derive explicit closed form solutions for continuous and discrete monetary streams. The mathematical method used is classical stochastic control theory.

Keywords: Portfolio optimisation, stochastic control, HJB equation, discretisation of control problems.

(23 pages, 2002)

32. M. Krekel

Optimal portfolios with a loan dependent credit spread

If an investor borrows money he generally has to pay higher interest rates than he would have received, if he had put his funds on a savings account. The classical model of continuous time portfolio optimisation ignores this effect. Since there is obviously a connection between the default probability and the total per-

centage of wealth, which the investor is in debt, we study portfolio optimisation with a control dependent interest rate. Assuming a logarithmic and a power utility function, respectively, we prove explicit formulae of the optimal control.
Keywords: Portfolio optimisation, stochastic control, HJB equation, credit spread, log utility, power utility, non-linear wealth dynamics
(25 pages, 2002)

33. J. Ohser, W. Nagel, K. Schladitz

The Euler number of discretized sets - on the choice of adjacency in homogeneous lattices

Two approaches for determining the Euler-Poincaré characteristic of a set observed on lattice points are considered in the context of image analysis { the integral geometric and the polyhedral approach. Information about the set is assumed to be available on lattice points only. In order to retain properties of the Euler number and to provide a good approximation of the true Euler number of the original set in the Euclidean space, the appropriate choice of adjacency in the lattice for the set and its background is crucial. Adjacencies are defined using tessellations of the whole space into polyhedrons. In R 3 , two new 14 adjacencies are introduced additionally to the well known 6 and 26 adjacencies. For the Euler number of a set and its complement, a consistency relation holds. Each of the pairs of adjacencies (14:1; 14:1), (14:2; 14:2), (6; 26), and (26; 6) is shown to be a pair of complementary adjacencies with respect to this relation. That is, the approximations of the Euler numbers are consistent if the set and its background (complement) are equipped with this pair of adjacencies. Furthermore, sufficient conditions for the correctness of the approximations of the Euler number are given. The analysis of selected microstructures and a simulation study illustrate how the estimated Euler number depends on the chosen adjacency. It also shows that there is not a uniquely best pair of adjacencies with respect to the estimation of the Euler number of a set in Euclidean space.
Keywords: image analysis, Euler number, neighborhod relationships, cuboidal lattice
(32 pages, 2002)

34. I. Ginzburg, K. Steiner

Lattice Boltzmann Model for Free-Surface flow and Its Application to Filling Process in Casting

A generalized lattice Boltzmann model to simulate free-surface is constructed in both two and three dimensions. The proposed model satisfies the interfacial boundary conditions accurately. A distinctive feature of the model is that the collision processes is carried out only on the points occupied partially or fully by the fluid. To maintain a sharp interfacial front, the method includes an anti-diffusion algorithm. The unknown distribution functions at the interfacial region are constructed according to the first order Chapman-Enskog analysis. The interfacial boundary conditions are satisfied exactly by the coefficients in the Chapman-Enskog expansion. The distribution functions are naturally expressed in the local interfacial coordinates. The macroscopic quantities at the interface are extracted from the least-square solutions of a locally linearized system obtained from the known distribution functions. The proposed method does not require any geometric front construction and is robust for any interfacial topology. Simulation results of realistic filling process are presented: rectangular cavity in two dimensions and Hammer box, Campbell box, Sheffield box, and Motorblock in three dimensions. To enhance the stability at high Reynolds numbers, various upwind-type schemes are developed. Free-slip and no-slip boundary conditions are also discussed.
Keywords: Lattice Boltzmann models; free-surface phenomena; interface boundary conditions; filling processes; injection molding; volume of fluid method; interface boundary conditions; advection-schemes; upwind-schemes
(54 pages, 2002)

35. M. Günther, A. Klar, T. Materne, R. Wegener

Multivalued fundamental diagrams and stop and go waves for continuum traffic equations

In the present paper a kinetic model for vehicular traffic leading to multivalued fundamental diagrams is developed and investigated in detail. For this model phase transitions can appear depending on the local density and velocity of the flow. A derivation of associated macroscopic traffic equations from the kinetic equation is given. Moreover, numerical experiments show the appearance of stop and go waves for highway traffic with a bottleneck.
Keywords: traffic flow, macroscopic equations, kinetic derivation, multivalued fundamental diagram, stop and go waves, phase transitions
(25 pages, 2002)

36. S. Feldmann, P. Lang, D. Prätzel-Wolters

Parameter influence on the zeros of network determinants

To a network N(q) with determinant D(s;q) depending on a parameter vector q Î Rr via identification of some of its vertices, a network N^ (q) is assigned. The paper deals with procedures to find N^ (q), such that its determinant D^ (s;q) admits a factorization in the determinants of appropriate subnetworks, and with the estimation of the deviation of the zeros of D^ from the zeros of D. To solve the estimation problem state space methods are applied.
Keywords: Networks, Equicofactor matrix polynomials, Realization theory, Matrix perturbation theory
(30 pages, 2002)

37. K. Koch, J. Ohser, K. Schladitz

Spectral theory for random closed sets and estimating the covariance via frequency space

A spectral theory for stationary random closed sets is developed and provided with a sound mathematical basis. Definition and proof of existence of the Bartlett spectrum of a stationary random closed set as well as the proof of a Wiener-Khintchine theorem for the power spectrum are used to two ends: First, well known second order characteristics like the covariance can be estimated faster than usual via frequency space. Second, the Bartlett spectrum and the power spectrum can be used as second order characteristics in frequency space. Examples show, that in some cases information about the random closed set is easier to obtain from these characteristics in frequency space than from their real world counterparts.
Keywords: Random set, Bartlett spectrum, fast Fourier transform, power spectrum
(28 pages, 2002)

38. D. d'Humières, I. Ginzburg

Multi-reflection boundary conditions for lattice Boltzmann models

We present a unified approach of several boundary conditions for lattice Boltzmann models. Its general framework is a generalization of previously introduced schemes such as the bounce-back rule, linear or quadratic interpolations, etc. The objectives are two fold: first to give theoretical tools to study the existing boundary conditions and their corresponding accuracy; secondly to design formally third- order accurate boundary conditions for general flows. Using these boundary conditions, Couette and Poiseuille flows are exact solution of the lattice Boltzmann models for a Reynolds number Re = 0 (Stokes limit).
Numerical comparisons are given for Stokes flows in periodic arrays of spheres and cylinders, linear periodic array of cylinders between moving plates and for Navier-Stokes flows in periodic arrays of cylinders for Re < 200. These results show a significant improvement of the overall accuracy when using the linear interpolations instead of the bounce-back reflection (up to an order of magnitude on the hydrodynamics fields). Further improvement is achieved with the new multi-reflection boundary conditions, reaching a level of accuracy close to the quasi-analytical reference solutions, even for rather modest grid resolutions and few points in the narrowest channels. More important, the pressure and velocity fields in the vicinity of the obstacles are much smoother with multi-reflection than with the other boundary conditions.
Finally the good stability of these schemes is highlighted by some simulations of moving obstacles: a cylinder between flat walls and a sphere in a cylinder.
Keywords: lattice Boltzmann equation, boudary condistions, bounce-back rule, Navier-Stokes equation
(72 pages, 2002)

39. R. Korn

Elementare Finanzmathematik

Im Rahmen dieser Arbeit soll eine elementar gehaltene Einführung in die Aufgabenstellungen und Prinzipien der modernen Finanzmathematik gegeben werden. Insbesondere werden die Grundlagen der Modellierung von Aktienkursen, der Bewertung von Optionen und der Portfolio-Optimierung vorgestellt. Natürlich können die verwendeten Methoden und die entwickelte Theorie nicht in voller Allgemeinheit für den Schulunterricht verwendet werden, doch sollen einzelne Prinzipien so heraus gearbeitet werden, dass sie auch an einfachen Beispielen verstanden werden können.
Keywords: Finanzmathematik, Aktien, Optionen, Portfolio-Optimierung, Börse, Lehrerweiterbildung, Mathematikunterricht
(98 pages, 2002)

40. J. Kallrath, M. C. Müller, S. Nickel

Batch Presorting Problems: Models and Complexity Results

In this paper we consider short term storage systems. We analyze presorting strategies to improve the effiency of these storage systems. The presorting task is called Batch PreSorting Problem (BPSP). The BPSP is a variation of an assigment problem, i. e., it has an assigment problem kernel and some additional constraints. We present different types of these presorting problems, introduce mathematical programming formulations and prove the NP-completeness for one type of the BPSP. Experiments are carried out in order to compare the different model formulations and to investigate the behavior of these models.
Keywords: Complexity theory, Integer programming, Assigment, Logistics
(19 pages, 2002)

41. J. Linn

On the frame-invariant description of the phase space of the Folgar-Tucker equation

The Folgar-Tucker equation is used in flow simulations of fiber suspensions to predict fiber orientation depending on the local flow. In this paper, a complete, frame-invariant description of the phase space of this differential equation is presented for the first time.
Key words: fiber orientation, Folgar-Tucker equation, injection molding
(5 pages, 2003)

42. T. Hanne, S. Nickel

A Multi-Objective Evolutionary Algorithm for Scheduling and Inspection Planning in Software Development Projects

In this article, we consider the problem of planning inspections and other tasks within a software development (SD) project with respect to the objectives quality (no. of defects), project duration, and costs. Based on a discrete-event simulation model of SD processes comprising the phases coding, inspection, test, and rework, we present a simplified formulation of the problem as a multiobjective optimization problem. For solving the problem (i. e. finding an approximation of the efficient set) we develop a multiobjective evolutionary algorithm. Details of the algorithm are discussed as well as results of its application to sample problems.
Key words: multiple objective programming, project management and scheduling, software development, evolutionary algorithms, efficient set
(29 pages, 2003)

43. T. Bortfeld , K.-H. Küfer, M. Monz, A. Scherrer, C. Thieke, H. Trinkaus

Intensity-Modulated Radiotherapy - A Large Scale Multi-Criteria Programming Problem -

Radiation therapy planning is always a tight rope walk between dangerous insufficient dose in the target volume and life threatening overdosing of organs at risk. Finding ideal balances between these inherently contradictory goals challenges dosimetrists and physicians in their daily practice. Today's planning systems are typically based on a single evaluation function that measures the quality of a radiation treatment plan. Unfortunately, such a one dimensional approach cannot satisfactorily map the different backgrounds of physicians and the patient dependent necessities. So, too often a time consuming iteration process between evaluation of dose distribution and redefinition of the evaluation function is needed.

In this paper we propose a generic multi-criteria approach based on Pareto's solution concept. For each entity of interest - target volume or organ at risk a structure dependent evaluation function is defined measuring deviations from ideal doses that are calculated from statistical functions. A reasonable bunch of clinically meaningful Pareto optimal solutions are stored in a data base, which can be interactively searched by physicians. The system guarantees dynamical planning as well as the discussion of tradeoffs between different entities.

Mathematically, we model the upcoming inverse problem as a multi-criteria linear programming problem. Because of the large scale nature of the problem it is not possible to solve the problem in a 3D-setting without adaptive reduction by appropriate approximation schemes.

Our approach is twofold: First, the discretization of the continuous problem is based on an adaptive hierarchical clustering process which is used for a local refinement of constraints during the optimization procedure. Second, the set of Pareto optimal solutions is approximated by an adaptive grid of representatives that are found by a hybrid process of calculating extreme compromises and interpolation methods.

Keywords: multiple criteria optimization, representative systems of Pareto solutions, adaptive triangulation, clustering and disaggregation techniques, visualization of Pareto solutions, medical physics, external beam radiotherapy planning, intensity modulated radiotherapy

(31 pages, 2003)

44. T. Halfmann, T. Wichmann

Overview of Symbolic Methods in Industrial Analog Circuit Design

Industrial analog circuits are usually designed using numerical simulation tools. To obtain a deeper circuit understanding, symbolic analysis techniques can additionally be applied. Approximation methods which reduce the complexity of symbolic expressions are needed in order to handle industrial-sized problems.

This paper will give an overview to the field of symbolic analog circuit analysis. Starting with a motivation, the state-of-the-art simplification algorithms for linear as well as for nonlinear circuits are presented. The basic ideas behind the different techniques are described, whereas the technical details can be found in the cited references. Finally, the application of linear and nonlinear symbolic analysis will be shown on two example circuits.

Keywords: CAD, automated analog circuit design, symbolic analysis, computer algebra, behavioral modeling, system simulation, circuit sizing, macro modeling, differential-algebraic equations, index

(17 pages, 2003)

45. S. E. Mikhailov, J. Orlik

Asymptotic Homogenisation in Strength and Fatigue Durability Analysis of Composites

Asymptotic homogenisation technique and two-scale convergence is used for analysis of macro-strength and fatigue durability of composites with a periodic structure under cyclic loading. The linear damage accumulation rule is employed in the phenomenological micro-durability conditions (for each component of the composite) under varying cyclic loading. Both local and non-local strength and durability conditions are analysed. The strong convergence of the strength and fatigue damage measure as the structure period tends to zero is proved and their limiting values are estimated.

Keywords: multiscale structures, asymptotic homogenization, strength, fatigue, singularity, non-local conditions

(14 pages, 2003)

46. P. Domínguez-Marín, P. Hansen, N. Mladenovi´c , S. Nickel

Heuristic Procedures for Solving the Discrete Ordered Median Problem

We present two heuristic methods for solving the Discrete Ordered Median Problem (DOMP), for which no such approaches have been developed so far. The DOMP generalizes classical discrete facility location problems, such as the p-median, p-center and Uncapacitated Facility Location problems. The first procedure proposed in this paper is based on a genetic algorithm developed by Moreno Vega [MV96] for p-median and p-center problems. Additionally, a second heuristic approach based on the Variable Neighborhood Search metaheuristic (VNS) proposed by Hansen & Mladenovic [HM97] for the p-median problem is described. An extensive numerical study is presented to show the efficiency of both heuristics and compare them.

Keywords: genetic algorithms, variable neighborhood search, discrete facility location

(31 pages, 2003)

47. N. Boland, P. Domínguez-Marín, S. Nickel, J. Puerto

Exact Procedures for Solving the Discrete Ordered Median Problem

The Discrete Ordered Median Problem (DOMP) generalizes classical discrete location problems, such as the N-median, N-center and Uncapacitated Facility Location problems. It was introduced by Nickel [16], who formulated it as both a nonlinear and a linear integer program. We propose an alternative integer linear programming formulation for the DOMP, discuss relationships between both integer linear programming formulations, and show how properties of optimal solutions can be used to strengthen these formulations. Moreover, we present a specific branch and bound procedure to solve the DOMP more efficiently. We test the integer linear programming formulations and this branch and bound method computationally on randomly generated test problems.

Keywords: discrete location, Integer programming

(41 pages, 2003)

48. S. Feldmann, P. Lang

Padé-like reduction of stable discrete linear systems preserving their stability

A new stability preserving model reduction algorithm for discrete linear SISO-systems based on their impulse response is proposed. Similar to the Padé approximation, an equation system for the Markov parameters involving the Hankel matrix is considered, that here however is chosen to be of very high dimension. Although this equation system therefore in general cannot be solved exactly, it is proved that the approximate solution, computed via the Moore-Penrose inverse, gives rise to a stability preserving reduction scheme, a property that cannot be guaranteed for the Padé approach. Furthermore, the proposed algorithm is compared to another stability preserving reduction approach, namely the balanced truncation method, showing comparable performance of the reduced systems. The balanced truncation method however starts from a state space description of the systems and in general is expected to be more computational demanding.

Keywords: Discrete linear systems, model reduction, stability, Hankel matrix, Stein equation

(16 pages, 2003)

49. J. Kallrath, S. Nickel

A Polynomial Case of the Batch Presorting Problem

This paper presents new theoretical results for a special case of the batch presorting problem (BPSP). We will show tht this case can be solved in polynomial time. Offline and online algorithms are presented for solving the BPSP. Competetive analysis is used for comparing the algorithms.

Keywords: batch presorting problem, online optimization, competetive analysis, polynomial algorithms, logistics

(17 pages, 2003)

50. T. Hanne, H. L. Trinkaus

knowCube for MCDM – Visual and Interactive Support for Multicriteria Decision Making

In this paper, we present a novel multicriteria decision support system (MCDSS), called knowCube, consisting of components for knowledge organization, generation, and navigation. Knowledge organization rests upon a database for managing qualitative and quantitative criteria, together with add-on information. Knowledge generation serves filling the database via e. g. identification, optimization, classification or simulation. For "finding needles in haycocks", the knowledge navigation component supports graphical database retrieval and interactive, goal-oriented problem solving. Navigation "helpers" are, for instance, cascading criteria aggregations, modifiable metrics, ergonomic interfaces, and customizable visualizations. Examples from real-life projects, e.g. in industrial engineering and in the life sciences, illustrate the application of our MCDSS.

Key words: Multicriteria decision making, knowledge management, decision support systems, visual interfaces, interactive navigation, real-life applications.

(26 pages, 2003)

51. O. Iliev, V. Laptev

On Numerical Simulation of Flow Through Oil Filters

This paper concerns numerical simulation of flow through oil filters. Oil filters consist of filter housing (filter box), and a porous filtering medium, which completely separates the inlet from the outlet. We discuss mathematical models, describing coupled flows in the pure liquid subregions and in the porous filter media, as well as interface conditions between them. Further, we reformulate the problem in fictitious regions method manner, and discuss peculiarities of the numerical algorithm in solving the coupled system. Next, we show numerical results, validating the model and the algorithm. Finally, we present results from simulation of 3-D oil flow through a real car filter.

Keywords: oil filters, coupled flow in plain and porous media, Navier-Stokes, Brinkman, numerical simulation

(8 pages, 2003)

52. W. Dörfler, O. Iliev, D. Stoyanov, D. Vassileva

On a Multigrid Adaptive Refinement Solver for Saturated Non-Newtonian Flow in Porous Media

A multigrid adaptive refinement algorithm for non-Newtonian flow in porous media is presented. The saturated flow of a non-Newtonian fluid is described by the continuity equation and the generalized Darcy law. The resulting second order nonlinear elliptic equation is discretized by a finite volume method on a cell-centered grid. A nonlinear full-multigrid, full-approximation-storage algorithm is implemented. As a smoother, a single grid solver based on Picard linearization and Gauss-Seidel relaxation is used. Further, a local refinement multigrid algorithm on a composite grid is developed. A residual based error indicator is used in the adaptive refinement criterion. A special implementation approach is used, which allows us to perform unstructured local refinement in conjunction with the finite volume discretization. Several results from numerical experiments are presented in order to examine the performance of the solver.

Keywords: Nonlinear multigrid, adaptive refinement, non-Newtonian flow in porous media

(17 pages, 2003)

53. S. Kruse

On the Pricing of Forward Starting Options under Stochastic Volatility

We consider the problem of pricing European forward starting options in the presence of stochastic volatility. By performing a change of measure using the asset price at the time of strike determination as a numeraire, we derive a closed-form solution based on Heston's model of stochastic volatility.

Keywords: Option pricing, forward starting options, Heston model, stochastic volatility, cliquet options

(11 pages, 2003)

54. O. Iliev, D. Stoyanov

Multigrid – adaptive local refinement solver for incompressible flows

A non-linear multigrid solver for incompressible Navier-Stokes equations, exploiting finite volume discretization of the equations, is extended by adaptive local refinement. The multigrid is the outer iterative cycle, while the SIMPLE algorithm is used as a smoothing procedure. Error indicators are used to define the refinement subdomain. A special implementation approach is used, which allows to perform unstructured local refinement in conjunction with the finite volume discretization. The multigrid - adaptive local refinement algorithm is tested on 2D Poisson equation and further is applied to a lid-driven flows in a cavity (2D and 3D case), comparing the results with bench-mark data. The software design principles of the solver are also discussed.

Keywords: Navier-Stokes equations, incompressible flow, projection-type splitting, SIMPLE, multigrid methods, adaptive local refinement, lid-driven flow in a cavity

(37 pages, 2003)

55. V. Starikovicius

The multiphase flow and heat transfer in porous media

In first part of this work, summaries of traditional Multiphase Flow Model and more recent Multiphase Mixture Model are presented. Attention is being paid to attempts include various heterogeneous aspects into models. In second part, MMM based differential model for two-phase immiscible flow in porous media is considered. A numerical scheme based on the sequential solution procedure and control volume based finite difference schemes for the pressure and saturation-conservation equations is developed. A computer simulator is built, which exploits object-oriented programming techniques. Numerical result for several test problems are reported.

Keywords: Two-phase flow in porous media, various formulations, global pressure, multiphase mixture model, numerical simulation

(30 pages, 2003)

56. P. Lang, A. Sarishvili, A. Wirsen

Blocked neural networks for knowledge extraction in the software development process

One of the main goals of an organization developing software is to increase the quality of the software while at the same time to decrease the costs and the duration of the development process. To achieve this, various decisions e.ecting this goal before and during the development process have to be made by the managers. One appropriate tool for decision support are simulation models of the software life cycle, which also help to understand the dynamics of the software development process. Building up a simulation model requires a mathematical description of the interactions between di.erent objects involved in the development process. Based on experimental data, techniques from the .eld of knowledge discovery can be used to quantify these interactions and to generate new process knowledge based on the analysis of the determined relationships. In this paper blocked neuronal networks and related relevance measures will be presented as an appropriate tool for quanti.cation and validation of qualitatively known dependencies in the software development process.

Keywords: Blocked Neural Networks, Nonlinear Regression, Knowledge Extraction, Code Inspection

(21 pages, 2003)

57. H. Knaf, P. Lang, S. Zeiser

Diagnosis aiding in Regulation Thermography using Fuzzy Logic

The objective of the present article is to give an overview of an application of Fuzzy Logic in Regulation Thermography, a method of medical diagnosis support. An introduction to this method of the complementary medical science based on temperature measurements – so-called thermograms – is provided. The process of modelling the physician's thermogram evaluation rules using the calculus of Fuzzy Logic is explained.

Keywords: fuzzy logic,knowledge representation, expert system

(22 pages, 2003)

58. M.T. Melo, S. Nickel, F. Saldanha da Gama

Largescale models for dynamic multi-commodity capacitated facility location

In this paper we focus on the strategic design of supply chain networks. We propose a mathematical modeling framework that captures many practical aspects of network design problems simultaneously but which have not received adequate attention in the literature. The aspects considered include: dynamic planning horizon, generic supply chain network structure, external supply of materials, inventory opportunities for goods, distribution of commodities, facility configuration, availability of capital for investments, and storage limitations. Moreover, network configuration decisions concerning the gradual relocation of facilities over the planning horizon are considered. To cope with fluctuating demands, capacity expansion and reduction scenarios are also analyzed as well as modular capacity shifts. The relation of the proposed modeling framework with existing models is discussed. For problems of reasonable size we report on our computational experience with standard mathematical programming software. In particular, useful insights on the impact of various factors on network design decisions are provided.

Keywords: supply chain management, strategic planning, dynamic location, modeling

(40 pages, 2003)

59. J. Orlik

Homogenization for contact problems with periodically rough surfaces

We consider the contact of two elastic bodies with rough surfaces at the interface. The size of the micro-peaks and valleys is very small compared with the macrosize of the bodies' domains. This makes the direct application of the FEM for the calculation of the contact problem prohibitively costly. A method is developed that allows deriving a macrocontact condition on the interface. The method involves the twoscale asymptotic homogenization procedure that takes into account the microgeometry of the interface layer and the stiffnesses of materials of both domains. The macrocontact condition can then be used in a FEM model for the contact problem on the macrolevel. The averaged contact stiffness obtained allows the replacement of the interface layer in the macromodel by the macrocontact condition.

Keywords: asymptotic homogenization, contact problems

(28 pages, 2004)

60. A. Scherrer, K.-H. Küfer, M. Monz, F. Alonso, T. Bortfeld

IMRT planning on adaptive volume structures – a significant advance of computational complexity

In intensity-modulated radiotherapy (IMRT) planning the oncologist faces the challenging task of finding a treatment plan that he considers to be an ideal compromise of the inherently contradictive goals of delivering a sufficiently high dose to the target while widely sparing critical structures. The search for this a priori unknown compromise typically requires the computation of several plans, i.e. the solution of several optimization problems. This accumulates to a high computational expense due to the large scale of these problems - a consequence of the discrete problem formulation. This paper presents the adaptive clustering method as a new algorithmic concept to overcome these difficulties. The computations are performed on an individually adapted structure of voxel clusters rather than on the original voxels leading to a decisively reduced computational complexity as numerical examples on real clinical data demonstrate. In contrast to many other similar concepts, the typical trade-off between a reduction in computational complexity and a loss in exactness can be avoided: the adaptive clustering method produces the optimum of the original problem. This flexible method can be applied to both single- and multi-criteria optimization methods based on most of the convex evaluation functions used in practice.

Keywords: Intensity-modulated radiation therapy (IMRT), inverse treatment planning, adaptive volume structures, hierarchical clustering, local refinement, adaptive clustering, convex programming, mesh generation, multi-grid methods

(24 pages, 2004)

61. D. Kehrwald

Parallel lattice Boltzmann simulation of complex flows

After a short introduction to the basic ideas of lattice Boltzmann methods and a brief description of a modern parallel computer, it is shown how lattice Boltzmann schemes are successfully applied for simulating fluid flow in microstructures and calculating material properties of porous media. It is explained how lattice Boltzmann schemes compute the gradient of the velocity field without numerical differentiation. This feature is then utilised for the simulation of pseudo-plastic fluids, and numerical results are presented for a simple benchmark problem as well as for the simulation of liquid composite moulding.

Keywords: Lattice Boltzmann methods, parallel computing, microstructure simulation, virtual material design, pseudo-plastic fluids, liquid composite moulding

(12 pages, 2004)

62. O. Iliev, J. Linn, M. Moog, D. Niedziela, V. Starikovicius

On the Performance of Certain Iterative Solvers for Coupled Systems Arising in Discretization of Non-Newtonian Flow Equations

Iterative solution of large scale systems arising after discretization and linearization of the unsteady non-Newtonian Navier–Stokes equations is studied. cross WLF model is used to account for the non-Newtonian behavior of the fluid. Finite volume method is used to discretize the governing system of PDEs. Viscosity is treated explicitely (e.g., it is taken from the previous time step), while other terms are treated implicitly. Different preconditioners (block–diagonal, block–triangular, relaxed incomplete LU factorization, etc.) are used in conjunction with advanced iterative methods, namely, BiCGStab, CGS, GMRES. The action of the preconditioner in fact requires inverting different blocks. For this purpose, in addition to preconditioned BiCGStab, CGS, GMRES, we use also algebraic multigrid method (AMG). The performance of the iterative solvers is studied with respect to the number of unknowns, characteristic velocity in the basic flow, time step, deviation from Newtonian behavior, etc. Results from numerical experiments are presented and discussed.

Keywords: Performance of iterative solvers, Preconditioners, Non-Newtonian flow

(17 pages, 2004)

63. R. Ciegis, O. Iliev, S. Rief, K. Steiner

On Modelling and Simulation of Different Regimes for Liquid Polymer Moulding

In this paper we consider numerical algorithms for solving a system of nonlinear PDEs arising in modeling of liquid polymer injection. We investigate the particular case when a porous preform is located within the mould, so that the liquid polymer flows through a porous medium during the filling stage. The nonlinearity of the governing system of PDEs is due to the non-Newtonian behavior of the polymer, as well as due to the moving free boundary. The latter is related to the penetration front and a Stefan type problem is formulated to account for it. A finite-volume method is used to approximate the given differential problem. Results

of numerical experiments are presented.
We also solve an inverse problem and present algorithms for the determination of the absolute preform permeability coefficient in the case when the velocity of the penetration front is known from measurements. In both cases (direct and inverse problems) we emphasize on the specifics related to the non-Newtonian behavior of the polymer. For completeness, we discuss also the Newtonian case. Results of some experimental measurements are presented and discussed.
Keywords: Liquid Polymer Moulding, Modelling, Simulation, Infiltration, Front Propagation, non-Newtonian flow in porous media
(43 pages, 2004)

64. T. Hanne, H. Neu

Simulating Human Resources in Software Development Processes

In this paper, we discuss approaches related to the explicit modeling of human beings in software development processes. While in most older simulation models of software development processes, esp. those of the system dynamics type, humans are only represented as a labor pool, more recent models of the discrete-event simulation type require representations of individual humans. In that case, particularities regarding the person become more relevant. These individual effects are either considered as stochastic variations of productivity, or an explanation is sought based on individual characteristics, such as skills for instance. In this paper, we explore such possibilities by recurring to some basic results in psychology, sociology, and labor science. Various specific models for representing human effects in software process simulation are discussed.
Keywords: Human resource modeling, software process, productivity, human factors, learning curve
(14 pages, 2004)

65. O. Iliev, A. Mikelic, P. Popov

Fluid structure interaction problems in deformable porous media: Toward permeability of deformable porous media

In this work the problem of fluid flow in deformable porous media is studied. First, the stationary fluid-structure interaction (FSI) problem is formulated in terms of incompressible Newtonian fluid and a linearized elastic solid. The flow is assumed to be characterized by very low Reynolds number and is described by the Stokes equations. The strains in the solid are small allowing for the solid to be described by the Lame equations, but no restrictions are applied on the magnitude of the displacements leading to strongly coupled, nonlinear fluid-structure problem. The FSI problem is then solved numerically by an iterative procedure which solves sequentially fluid and solid subproblems. Each of the two subproblems is discretized by finite elements and the fluid-structure coupling is reduced to an interface boundary condition. Several numerical examples are presented and the results from the numerical computations are used to perform permeability computations for different geometries.
Keywords: fluid-structure interaction, deformable porous media, upscaling, linear elasticity, stokes, finite elements
(28 pages, 2004)

66. F. Gaspar, O. Iliev, F. Lisbona, A. Naumovich, P. Vabishchevich

On numerical solution of 1-D poroelasticity equations in a multilayered domain

Finite volume discretization of Biot system of poroelasticity in a multilayered domain is presented. Staggered grid is used in order to avoid nonphysical oscillations of the numerical solution, appearing when a collocated grid is used. Various numerical experiments are presented in order to illustrate the accuracy of the finite difference scheme. In the first group of experiments, problems having analytical solutions are solved, and the order of convergence for the velocity, the pressure, the displacements, and the stresses is analyzed. In the second group of experiments numerical solution of real problems is presented.
Keywords: poroelasticity, multilayered material, finite volume discretization, MAC type grid
(41 pages, 2004)

67. J. Ohser, K. Schladitz, K. Koch, M. Nöthe

Diffraction by image processing and its application in materials science

A spectral theory for constituents of macroscopically homogeneous random microstructures modeled as homogeneous random closed sets is developed and provided with a sound mathematical basis, where the spectrum obtained by Fourier methods corresponds to the angular intensity distribution of x-rays scattered by this constituent. It is shown that the fast Fourier transform applied to three-dimensional images of microstructures obtained by micro-tomography is a powerful tool of image processing. The applicability of this technique is is demonstrated in the analysis of images of porous media.
Keywords: porous microstructure, image analysis, random set, fast Fourier transform, power spectrum, Bartlett spectrum
(13 pages, 2004)

68. H. Neunzert

Mathematics as a Technology: Challenges for the next 10 Years

No doubt: Mathematics has become a technology in its own right, maybe even a key technology. Technology may be defined as the application of science to the problems of commerce and industry. And science? Science maybe defined as developing, testing and improving models for the prediction of system behavior; the language used to describe these models is mathematics and mathematics provides methods to evaluate these models. Here we are! Why has mathematics become a technology only recently? Since it got a tool, a tool to evaluate complex, "near to reality" models: Computer! The model may be quite old – Navier-Stokes equations describe flow behavior rather well, but to solve these equations for realistic geometry and higher Reynolds numbers with sufficient precision is even for powerful parallel computing a real challenge. Make the models as simple as possible, as complex as necessary – and then evaluate them with the help of efficient and reliable algorithms: These are genuine mathematical tasks.
Keywords: applied mathematics, technology, modelling, simulation, visualization, optimization, glass processing, spinning processes, fiber-fluid interaction, trubulence effects, topological optimization, multicriteria optimization, Uncertainty and Risk, financial mathematics, Malliavin calculus, Monte-Carlo methods, virtual material design, filtration, bio-informatics, system biology
(29 pages, 2004)

69. R. Ewing, O. Iliev, R. Lazarov, A. Naumovich

On convergence of certain finite difference discretizations for 1D poroelasticity interface problems

Finite difference discretizations of 1D poroelasticity equations with discontinuous coefficients are analyzed. A recently suggested FD discretization of poroelasticity equations with constant coefficients on staggered grid, [5], is used as a basis. A careful treatment of the interfaces leads to harmonic averaging of the discontinuous coefficients. Here, convergence for the pressure and for the displacement is proven in certain norms for the scheme with harmonic averaging (HA). Order of convergence 1.5 is proven for arbitrary located interface, and second order convergence is proven for the case when the interface coincides with a grid node. Furthermore, following the ideas from [3], modified HA discretization are suggested for particular cases. The velocity and the stress are approximated with second order on the interface in this case. It is shown that for wide class of problems, the modified discretization provides better accuracy. Second order convergence for modified scheme is proven for the case when the interface coincides with a displacement grid node. Numerical experiments are presented in order to illustrate our considerations.
Keywords: poroelasticity, multilayered material, finite volume discretizations, MAC type grid, error estimates
(26 pages,2004)

70. W. Dörfler, O. Iliev, D. Stoyanov, D. Vassileva

On Efficient Simulation of Non-Newtonian Flow in Saturated Porous Media with a Multigrid Adaptive Refinement Solver

Flow of non-Newtonian in saturated porous media can be described by the continuity equation and the generalized Darcy law. Efficient solution of the resulting second order nonlinear elliptic equation is discussed here. The equation is discretized by a finite volume method on a cell-centered grid. Local adaptive refinement of the grid is introduced in order to reduce the number of unknowns. A special implementation approach is used, which allows us to perform unstructured local refinement in conjunction with the finite volume discretization. Two residual based error indicators are exploited in the adaptive refinement criterion. Second order accurate discretization on the interfaces between refined and non-refined subdomains, as well as on the boundaries with Dirichlet boundary condition, are presented here, as an essential part of the accurate and efficient algorithm. A nonlinear full approximation storage multigrid algorithm is developed especially for the above described composite (coarse plus locally refined) grid approach. In particular, second order approximation around interfaces is a result of a quadratic approximation of slave nodes in the multigrid - adaptive refinement (MG-AR) algorithm. Results from numerical solution of various academic and practice-induced problems are presented and the performance of the solver is discussed.
Keywords: Nonlinear multigrid, adaptive renement, non-Newtonian in porous media
(25 pages, 2004)

71. J. Kalcsics, S. Nickel, M. Schröder

Towards a Unified Territory Design Approach – Applications, Algorithms and GIS Integration

Territory design may be viewed as the problem of grouping small geographic areas into larger geographic clusters called territories in such a way that the latter are acceptable according to relevant planning criteria. In this paper we review the existing literature for applications of territory design problems and solution approaches for solving these types of problems. After identifying features common to all applications we introduce a basic territory design model and present in detail two approaches for solving this model: a classical location–allocation approach combined with optimal split resolution techniques and a newly developed computational geometry based method. We present computational results indicating the efficiency and suitability of the latter method for solving large–scale practical problems in an interactive environment. Furthermore, we discuss extensions to the basic model and its integration into Geographic Information Systems.
Keywords: territory desgin, political districting, sales territory alignment, optimization algorithms, Geographical Information Systems
(40 pages, 2005)

72. K. Schladitz, S. Peters, D. Reinel-Bitzer, A. Wiegmann, J. Ohser

Design of acoustic trim based on geometric modeling and flow simulation for non-woven

In order to optimize the acoustic properties of a stacked fiber non-woven, the microstructure of the non-woven is modeled by a macroscopically homogeneous random system of straight cylinders (tubes). That is, the fibers are modeled by a spatially stationary random system of lines (Poisson line process), dilated by a sphere. Pressing the non-woven causes anisotropy. In our model, this anisotropy is described by a one parametric distribution of the direction of the fibers. In the present application, the anisotropy parameter has to be estimated from 2d reflected light microscopic images of microsections of the non-woven.
After fitting the model, the flow is computed in digitized realizations of the stochastic geometric model using the lattice Boltzmann method. Based on the flow resistivity, the formulas of Delany and Bazley predict the frequency-dependent acoustic absorption of the non-woven in the impedance tube.

Using the geometric model, the description of a non-woven with improved acoustic absorption properties is obtained in the following way: First, the fiber thicknesses, porosity and anisotropy of the fiber system are modified. Then the flow and acoustics simulations are performed in the new sample. These two steps are repeatedc for various sets of parameters. Finally, the set of parameters for the geometric model leading to the best acoustic absorption is chosen.
Keywords: random system of fibers, Poisson line process, flow resistivity, acoustic absorption, Lattice-Boltzmann method, non-woven
(21 pages, 2005)

73. V. Rutka, A. Wiegmann

Explicit Jump Immersed Interface Method for virtual material design of the effective elastic moduli of composite materials

Virtual material design is the microscopic variation of materials in the computer, followed by the numerical evaluation of the effect of this variation on the material's macroscopic properties. The goal of this procedure is an in some sense improved material. Here, we give examples regarding the dependence of the effective elastic moduli of a composite material on the geometry of the shape of an inclusion. A new approach on how to solve such interface problems avoids mesh generation and gives second order accurate results even in the vicinity of the interface.
The Explicit Jump Immersed Interface Method is a finite difference method for elliptic partial differential equations that works on an equidistant Cartesian grid in spite of non-grid aligned discontinuities in equation parameters and solution. Near discontinuities, the standard finite difference approximations are modified by adding correction terms that involve jumps in the function and its derivatives. This work derives the correction terms for two dimensional linear elasticity with piecewise constant coefficients, i. e. for composite materials. It demonstrates numerically convergence and approximation properties of the method.
Keywords: virtual material design, explicit jump immersed interface method, effective elastic moduli, composite materials
(22 pages, 2005)

74. T. Hanne

Eine Übersicht zum Scheduling von Baustellen

Im diesem Dokument werden Aspekte der formalen zeitlichen Planung bzw. des Scheduling für Bauprojekte anhand ausgewählter Literatur diskutiert. Auf allgemeine Aspekte des Scheduling soll dabei nicht eingegangen werden. Hierzu seien als Standard-Referenzen nur Brucker (2004) und Pinedo (1995) genannt. Zu allgemeinen Fragen des Projekt-Managements sei auf Kerzner (2003) verwiesen.
Im Abschnitt 1 werden einige Anforderungen und Besonderheiten der Planung von Baustellen diskutiert. Diese treten allerdings auch in zahlreichen anderen Bereichen der Produktionsplanung und des Projektmanagements auf. In Abschnitt 2 werden dann Aspekte zur Formalisierung von Scheduling-Problemen in der Bauwirtschaft diskutiert, insbesondere Ziele und zu berücksichtigende Restriktionen. Auf eine mathematische Formalisierung wird dabei allerdings verzichtet. Abschnitt 3 bietet eine Übersicht über Verfahren und grundlegende Techniken für die Berechnung von Schedules. In Abschnitt 4 wird ein Überblick über vorhandene Software, zum einen verbreitete Internationale Software, zum anderen deutschsprachige Branchenlösungen, gegeben. Anschließend werden Schlussfolgerungen gezogen und es erfolgt eine Auflistung der Literaturquellen.
Keywords: Projektplanung, Scheduling, Bauplanung, Bauindustrie
(32 pages, 2005)

75. J. Linn

The Folgar–Tucker Model as a Differential Algebraic System for Fiber Orientation Calculation

The Folgar–Tucker equation (FTE) is the model most frequently used for the prediction of fiber orientation (FO) in simulations of the injection molding process for short–fiber reinforced thermoplasts. In contrast to its widespread use in injection molding simulations, little is known about the mathematical properties of the FTE: an investigation of e. g. its phase space M_{FT} has been presented only recently [12]. The restriction of the dependent variable of the FTE to the set M_{FT} turns the FTE into a differential algebraic system (DAS), a fact which is commonly neglected when devising numerical schemes for the integration of the FTE. In this article we present some recent results on the problem of trace stability as well as some introductory material which complements our recent paper [12].
Keywords: fiber orientation, Folgar–Tucker model, invariants, algebraic constraints, phase space, trace stability
(15 pages, 2005)

76. M. Speckert, K. Dreßler, H. Mauch, A. Lion, G. J. Wierda

Simulation eines neuartigen Prüfsystems für Achserprobungen durch MKS-Modellierung einschließlich Regelung

Testing new suspensions based on real load data is performed on elaborate multi channel test rigs. Usually, wheel forces and moments measured during driving maneuvers are reproduced by the test rig. Because of the complicated interaction between test rig and suspension each new rig configuration has to prove its efficiency with respect to the requirements and the configuration might be subject to optimization.
This paper deals with mathematical and physical modeling of a new concept of a test rig which is based on two hexapods. The model contains the geometric configuration as well as the hydraulics and the controller. It is implemented as an ADAMS/Car template and can be combined with different suspension models to get a complete assembly representing the entire test rig. Using this model, all steps required for a real test run such as controller adaptation, drive file iteration and simulation can be performed. Geometric or hydraulic parameters can be modified easily to improve the setup and adapt the system to the suspension and the given load data.
The model supports and accompanies the introduction of the new rig concept and can be used to prepare real tests on a virtual basis. Using both a front and a rear suspension the approach is described and the potentials coming with the simulation are pointed out.
Keywords: virtual test rig, suspension testing, multibody simulation, modeling hexapod test rig, optimization of test rig configuration
(20 pages, 2005)
In deutscher Sprache; bereits erschienen in: VDI-Berichte Nr. 1900, VDI-Verlag GmbH Düsseldorf (2005), Seiten 227-246

77. K.-H. Küfer, M. Monz, A. Scherrer, P. Süss, F. Alonso, A. S. A. Sultan, Th. Bortfeld, D. Craft, Chr. Thieke

Multicriteria optimization in intensity modulated radiotherapy planning

Inverse treatment planning of intensity modulated radiothrapy is a multicriteria optimization problem: planners have to find optimal compromises between a sufficiently highdose intumor tissuethat garantuee a high tumor control, and, dangerous overdosing of critical structures, in order to avoid high normal tissue complcication problems.
The approach presented in this work demonstrates how to state a flexible generic multicriteria model of the IMRT planning problem and how to produce clinically highly relevant Pareto-solutions. The model is imbedded in a principal concept of Reverse Engineering, a general optimization paradigm for design problems. Relevant parts of the Pareto-set are approximated by using extreme compromises as cornerstone solutions, a concept that is always feasible if box constraints for objective funtions are available. A major practical drawback of generic multicriteria concepts trying to compute or approximate parts of the Pareto-set is the high computational effort. This problem can be overcome by exploitation of an inherent asymmetry of the IMRT planning problem and an adaptive approximation scheme for optimal solutions based on an adaptive clustering preprocessing technique. Finally, a coherent approach for calculating and selecting solutions in a real-timeinteractive decision-making process is presented. The paper is concluded with clinical examples and a discussion of ongoing research topics.
Keywords: multicriteria optimization, extreme solutions, real-time decision making, adaptive approximation schemes, clustering methods, IMRT planning, reverse engineering
(51 pages, 2005)

78. S. Amstutz, H. Andrä

A new algorithm for topology optimization using a level-set method

The levelset method has been recently introduced in the field of shape optimization, enabling a smooth representation of the boundaries on a fixed mesh and therefore leading to fast numerical algorithms. However, most of these algorithms use a HamiltonJacobi equation to connect the evolution of the levelset function with the deformation of the contours, and consequently they cannot create any new holes in the domain (at least in 2D). In this work, we propose an evolution equation for the levelset function based on a generalization of the concept of topological gradient. This results in a new algorithm allowing for all kinds of topology changes.
Keywords: shape optimization, topology optimization, topological sensitivity, level-set
(22 pages, 2005)

79. N. Ettrich

Generation of surface elevation models for urban drainage simulation

Traditional methods fail for the purpose of simulating the complete flow process in urban areas as a consequence of heavy rainfall and as required by the European Standard EN-752 since the bi-directional coupling between sewer and surface is not properly handled. The methodology, developed in the BMBF/EUREKA-project RisUrSim, solves this problem by carrying out the runoff on the basis of shallow water equations solved on high-resolution surface grids. Exchange nodes between the sewer and the surface, like inlets and manholes, are located in the computational grid and water leaving the sewer in case of surcharge is further distributed on the surface.
So far, it has been a problem to get the dense topographical information needed to build models suitable for hydrodynamic runoff calculation in urban areas. Recent airborne data collection methods like laser scanning, however, offer a great chance to economically gather densely sampled input data. This paper studies the potential of such laser-scan data sets for urban water hydrodynamics.
Keywords: Flooding, simulation, urban elevation models, laser scanning
(22 pages, 2005)

80. H. Andrä, J. Linn, I. Matei, I. Shklyar, K. Steiner, E. Teichmann

OPTCAST – Entwicklung adäquater Strukturoptimierungsverfahren für Gießereien Technischer Bericht (KURZFASSUNG)

Im vorliegenden Bericht werden die Erfahrungen und Ergebnisse aus dem Projekt **OptCast** zusammengestellt. Das Ziel dieses Projekts bestand (a) in der Anpassung der Methodik der automatischen Strukturoptimierung für Gussteile und (b) in der Entwicklung und Bereitstellung von gießereispezifischen Optimierungstools für Gießereien und Ingenieurbüros.
Gießtechnische Restriktionen lassen sich nicht auf geometrische Restriktionen reduzieren, sondern sind nur über eine Gießsimulation (Erstarrungssimulation und Eigenspannungsanalyse) adäquat erfassbar, da die lokalen Materialeigenschaften des Gussteils nicht nur von der geometrischen Form des Teils, sondern auch vom verwendeten Material abhängen. Wegen dieser Erkenntnis wurde ein neuartiges iteratives Topologieoptimierungsverfahren unter Verwendung der Level-Set-Technik entwickelt, bei dem keine variable Dichte des Materials eingeführt wird. In jeder Iteration wird ein scharfer Rand des Bauteils berechnet. Somit ist die Gießsimulation in den iterativen Optimierungsprozess integrierbar.
Der Bericht ist wie folgt aufgebaut: In Abschnitt 2 wird der Anforderungskatalog erläutert, der sich aus der Bearbeitung von Benchmark-Problemen in der ersten Projektphase ergab. In Abschnitt 3 werden die Benchmark-Probleme und deren Lösung mit den im Projekt

entwickelten Tools beschrieben. Abschnitt 4 enthält die Beschreibung der neu entwickelten Schnittstellen und die mathematische Formulierung des Topologieoptimierungsproblems. Im letzten Abschnitt wird das neue Topologieoptimierungsverfahren, das die Simulation des Gießprozesses einschließt, erläutert.
Keywords: Topologieoptimierung, Level-Set-Methode, Gießprozesssimulation, Gießtechnische Restriktionen, CAE-Kette zur Strukturoptimierung
(77 pages, 2005)

81. N. Marheineke, R. Wegener

Fiber Dynamics in Turbulent Flows
Part I: General Modeling Framework

The paper at hand deals with the modeling of turbulence effects on the dynamics of a long slender elastic fiber. Independent of the choice of the drag model, a general aerodynamic force concept is derived on the basis of the velocity field for the randomly fluctuating component of the flow. Its construction as centered differentiable Gaussian field complies thereby with the requirements of the stochastic k-ε turbulence model and Kolmogorov's universal equilibrium theory on local isotropy.
Keywords: fiber-fluid interaction; Cosserat rod; turbulence modeling; Kolmogorov's energy spectrum; double-velocity correlations; differentiable Gaussian fields

Part II: Specific Taylor Drag

In [12], an aerodynamic force concept for a general air drag model is derived on top of a stochastic k-ε description for a turbulent flow field. The turbulence effects on the dynamics of a long slender elastic fiber are particularly modeled by a correlated random Gaussian force and in its asymptotic limit on a macroscopic fiber scale by Gaussian white noise with flow-dependent amplitude. The paper at hand now presents quantitative similarity estimates and numerical comparisons for the concrete choice of a Taylor drag model in a given application.
Keywords: flexible fibers; k-ε turbulence model; fiber-turbulence interaction scales; air drag; random Gaussian aerodynamic force; white noise; stochastic differential equations; ARMA process
(38 pages, 2005)

82. C. H. Lampert, O. Wirjadi

An Optimal Non-Orthogonal Separation of the Anisotropic Gaussian Convolution Filter

We give ananalytical and geometrical treatment of what it means to separate a Gaussian kernel along arbitrary axes in R^n, and we present a separation scheme that allows to efficiently implement anisotropic Gaussian convolution filters in arbitrary dimension. Based on our previous analysis we show that this scheme is optimal with regard to the number of memory accesses and interpolation operations needed.
Our method relies on non-orthogonal convolution axes and works completely in image space. Thus, it avoids the need for an FFT-subroutine. Depending on the accuracy and speed requirements, different interpolation schemes and methods to implement the one-dimensional Gaussian (FIR, IIR) can be integrated. The algorithm is also feasible for hardware that does not contain a floating-point unit.
Special emphasis is laid on analyzing the performance and accuracy of our method. In particular, we show that without anyspecial optimization of the source code, our method can perform anisotropic Gaussian filtering faster than methods relying on the Fast Fourier Transform.
Keywords: Anisotropic Gaussian filter, linear filtering, orientation space, nD image processing, separable filters
(25 pages, 2005)

Status quo: November 2005